Asian Journal of Chemistry; Vol. 38, No. 3 (2026), 561-581
ASIAN JOURNAL OF CHEMISTRY
https://doi.org/10.14233/ajchem.2026.35352

REVIEW

A Comprehensive Review on Pyrazole Derivatives as Inhibitors for Iron Protection in Acidic Media: From Molecular Interactions to Corrosion Control

N. PUNITHA[1,*], A. SIVAKUMAR[1], A. PARVATHI PRIYA[2], M. ANITHA[1] and A. THAMIZHANBAN[3]

[1]PG and Research Department of Chemistry, Rajah Serfoji Government College (Autonomous) (Affiliated to Bharathidasan University, Thiruchirappalli), Thanjavur-613005, India
[2]Department of Science and Humanities, R.M.K. Engineering College, Thiruvallur-601206, Chennai, India
[3]Department of Chemistry, Thiru. Vi. Ka. Government Arts College (Affiliated to Bharathidasan University, Thiruchirappalli), Thiruvarur-610003, India

*Corresponding author: E-mail: npunithachem23@gmail.com

Received: 28 November 2025 *Accepted*: 4 February 2026 *Published online*: 6 March 2026 AJC-22275

Corrosion in industrial systems represents a major economic and technical challenge, resulting in annual global losses amounting to several billions of dollars. To mitigate the severe economic and structural impacts of corrosion, researchers are developing efficient and environmentally acceptable inhibitors for metallic materials. Both organic and inorganic inhibitors have been extensively studied for their ability to retard metal degradation in aggressive environments through surface adsorption or passive film formation. Laboratory research had already employed various methods, together with weight loss (WL), potentiodynamic polarisation (PDP) and electrochemical impedance (EIS), to address the issue by 1995. These techniques were implemented through experiments. Atomic force spectroscopy (AFM), scanning electron microscope (SEM) and energy dispersive spectrum (EDX) also utilised as supportive evidence. A focus was placed on organic inhibitors containing heteroatoms as well as extracts/oils from plants. This comprehensive review aims to summarize the recent research status of the compounds containing pyrazole moiety as corrosion protectors for Fe metal in a hydrochloric acid (HCl) environment. There are literature data on corrosion inhibitors that contain these pyrazole derivatives that are used in acid solutions to protect steel. In addition to organic-metal ion complexes, compounds with pyrazole moieties adsorb on metallic surfaces by physical or chemical processes. In general, pyrazole molecules are capable of suppressing both anodic and cathodic corrosion. In the majority of the literature, researchers used the Gaussian 09 program to compare DFT theoretical results with experimental findings.

Keywords: Steel, Pyrazoles, Potentiodynamic polarisation, Electrochemical impedance, Hydrochloric acid, Corrosion inhibition.

INTRODUCTION

Metals constitute the structural foundation of industrialized societies, underpinning infrastructure, transportation, energy systems and manufacturing sectors. Their high mechanical strength, electrical and thermal conductivity, and long-term durability render them indispensable for sustained economic and technological advancement. From the earliest stages of civilization, metallurgical processing has marked a pivotal technological breakthrough and in the modern era, current lifestyle is virtually inconceivable without the pervasive application of metallic materials [1,2].

Among metallic materials, steel, primarily composed of iron, derives its enhanced mechanical and chemical characteristics from the controlled addition of carbon and other alloying elements [3]. Based on the carbon content, steel is generally classified into three categories: low (mild), medium and high carbon steel. Low carbon steel, containing approximately 0.04-0.30% carbon, is widely utilized due to its good ductility, weldability and moderate strength, with a melting temperature typically ranging between 1450-1520 ºC [4]. The ability to melt at high temperature increases its flexibility in applications like cutting, forging, welding, drilling and other processes. Owing to its low carbon content, the material exhibits enhanced formability, allowing it to be shaped into complex geometries with reduced risk of cracking or fracture. In contrast, medium carbon steel (containing a carbon percentage of 0.31 to 0.60) and carbon tool steel or high carbon steel

(with a carbon percentage of 0.61 to 1.50) exhibit greater strength than mild steel (MS), however, are very susceptible to breaking while bent or twisted. Other than carbon different elements are added to steel in order to enhance its properties like corrosion resistance, wear resistance, tensile strength *etc*. [5,6]. The unique properties of steel led to an increase in its demand and usage. Thus, chemical engineers use it to design reactors and tanks for the handling of corrosive liquids, such as acids, bases and salt solutions.

Descaling, acid pickling, acid cleaning and various petrochemical processes generally require acid solutions. Among the various acid solutions, HCl is most commonly used for the pickling process [7]. The acidic environment easily damages and corrodes the iron. The corrosion process involves a reaction between materials and their environment, which results in the destruction of these materials. Globally, corrosion has become a significant problem due of its serious consequences [8]. Besides everyday degradation, corrosion leads to plant closures, loss of valuable resources, contamination of products and reduces competence. It also causes costly maintenance and costly overdesign. As a result, safety risks rise and technological progress is hampered. Nowadays, the primary problem in any industry is reducing overall corrosion costs [9-12]. It is possible to control corrosion by recognizing the comprehended corrosion mechanisms and employing corrosion resistant materials.

Numerous studies have proven that the most efficient method to prevent metal corrosion is by utilizing corrosion inhibitors. Historically, several types of inhibitors have been widely accepted in various industries for its excellent anticorrosive properties. Organic or inorganic substances or mixtures are used to inhibit, prevent or minimize corrosion in an aggressive environment at low concentrations [13-18]. According to available information, mostly organic inhibitors work by adhering to the surface of metals. In recent years, heterocyclic compounds containing nitrogen have been demonstrated to be effective corrosion inhibitors for metals in acid medium [19].

Pyrazoles have recently attracted much attention as scaffolds for the development of novel molecules with a variety of distinct characteristics in the field of corrosion science. Due to their strong coordinating ability and tunable electronic characteristics, pyrazoles serve as effective ligands for various metal centres. The labile electron doublets of these nitrogen compounds make them excellent organic inhibitors of corrosion [20-22]. The main focus of this review is to discuss the effective application of pyrazole derivatives as organic corrosion inhibitors for metals in HCl environment.

Corrosion inhibition behaviour of heterocyclic compounds with one pyrazole moiety: According to potentiodynamic polarisation (PDP) study, pyrazole (**1**) inhibits the deterioration of iron in HCl with 70.34% of inhibition efficiency. The adsorption model of pyrazole follows Langmuir isotherm and performed as an anodic inhibitor [23]. Furthermore, the effectiveness of 1-methylpyrazole (**2**) in inhibiting iron deterioration in 1.0 M HCl medium was assessed at diverse concentrations. About 61.79% inhibition potential was observed for the inhibitor **2** in electrochemical experiment. The Temkin isotherm was found to explain the adsorption behaviour of compound **2** and anodic inhibition was confirmed by the Tafel curve [24]. The anticorrosion performance of 3,5-dimethyl-1*H*-pyrazole (**3**) on MS in 1.0 M HCl environment studied as only 39% inhibition efficiency, whereas the inhibition efficiency of compound **3** reached 83% for Armco iron in the same HCl medium. The Frumkin's isotherm model was predicted for inhibitor **3** absorption on iron [25,26].

Corrosion inhibition recital of three heterocyclic compounds containing pyrazole moiety such as (*E*)-5-(4-(dimethylamino)phenyl)-3-(4-(dimethylamino)styryl)-4,5-dihydro-1*H*-pyrazole-1-carboxamide (**4**), (*E*)-5-(4-(dimethylamino)-phenyl)-3-(4-(dimethylamino)styryl)-2,3-dihydro-1*H*-pyrazole-1-carbothioamide (**5**) and 5-(4-(dimethylamino)phenyl)-3-phenyl-4,5-dihydro-1*H*-pyrazole-1-carboxamide (**6**) on mild steel (MS) in HCl medium. The outcomes demonstrated that the studied pyrazoles **4**, **5** and **6** had an efficiency of 80% at 1.6×10^{-4}, 96.06% at 5×10^{-4} mol L^{-1} and 84.56% at 4×10^{-4}, respectively, at 303 K. The adsorption phenomenon of these inhibitors on the MS exterior displays the Langmuir model isotherm. Tafel curves divulge that all these inhibitors act as a mixed-kind protector and electrochemical impedance spectral (EIS) study shows the raise of inhibitors concentration with charge transfer resistance. The SEM characterisation confirmed the formation of protective film over the MS [27,28]. Similarly, the other two carbothioamide compounds with pyrazole moiety *viz*. 3,5-diphenyl-4,5-dihydro-1H-pyrazole-1-carbothioamide (**7**) and 5-(3-methoxyphenyl)-3-phenyl-4,5-dihydro-1*H*-pyrazole-1-carbothioamide (**8**) were synthesised as inhibitor for MS in acid solution. The inhibitors adsorbed on MS surface *via* Langmuir isothermal adsorption model. This adsorption involves two kinds of interactions such as chemisorption and physisorption. The outcomes revealed that the derivative **7** is less effective than **8** in HCl medium [29].

In accordance with electrochemical studies both 2-(((2,3-dihydro-1*H*-pyrazol-1yl)methyl)amino)pyrimidine-4,6-diol (**9**), 1-methyl-4-methylsulfanyl-1*H*-pyrazolo[3,4-*d*]pyrimidine (**10**) and 1-ethyl-1*H*-pyrazolo[3,4-*d*]pyrimidine-4(5*H*)-thione (**11**) are good mixed kind protector but predominantly inhibit cathodic corrosion. The corrosion hindrance effectiveness slightly decreases with increasing the temperature ranging from 303 to 343 K. The monolayer adsorption of inhibitors **10** and **11** on MS follow the Langmuir isotherm model. The activation factors designate the physisorption behaviour of inhibitors. The corrosion hindrance efficiency at the optimal concentration (10^{-3} M) was found to be >90% for both the compounds, however, compound **11** have high protecting efficiency than compound **10** [30,31].

Different experimental and theoretical approaches have been used to investigate the efficacy of two pyrazoline derivatives namely, 2-(4-(5-(*p*-tolyl)-4,5-dihydro-1*H*-pyrazol-3-yl)phenoxy)acetic acid (**12**) and 2-(4-(5-(4-nitrophenyl)-4,5-dihydro-1*H*-pyrazol-3-yl)phenoxy)acetic acid (**13**) as an inhibitor for MS in acid medium (1.0 M HCl) at 303 K [32]. These pyrazoline inhibitors exhibit inhibition efficiency of 89% and 92% in PDP technique for the compounds **12** and **13**, respectively. According to EIS, both derivatives act *via* mixed-kind corrosion hindrance mechanism. Their adsorption on MS was confirmed to obey Langmuir isothermal adsorption. Surface analysis using AFM and SEM demonstrated that the investigated compounds form a protective layer on the mild steel surface, thereby mitigating corrosion. Furthermore,

quantum chemical calculations and molecular dynamics simulations strongly support the experimental findings by confirming favourable adsorption and stable interaction of the inhibitors with the metal surface.

The anticorrosion activity of 1-{[benzyl-(2-cyano-ethyl)-amino]methyl}-5-methyl-1*H*-pyrazole-3-carboxylic acid ethyl ester (**14**) and 1-{[benzyl-(2-cyano-ethyl)-amino]-methyl}-5-methyl-1*H*-pyrazole-3-carboxylic acid methyl ester (**15**) on MS in HCl was also determined. An increase in temperature leads to a decrease in corrosion inhibition efficiency. The Langmuir kind isotherm model of adsorption was determined for both compounds **14** and **15** with 91.5% and 90.6% efficiencies, respectively from PDP method [33]. The concentration of 10^{-3} M increases the inhibition efficiencies to attain a maximum value.

Two novel derivatives of pyrazole, N-((3,5-dimethyl-1*H*-pyrazole-1-yl)methyl)pyridine-4-amine (**16**) and 4-(((3,5-dimethyl-1*H*-pyrazole-1-yl)methyl)amino)benzoic acid (**17**) were also examined as effective anticorrosive agent for MS in HCl [34]. Electrochemical experiments demonstrated that derivatives **16** and **17** exhibit mixed-type inhibitory activity with 96% and 93% inhibition efficiencies, respectively, at 10^{-3} M. Derivative **17** with benzoic acid showed a higher efficiency than **16**, which may be due to the elevated density of electrons on carboxyl group, as a strong bond with the MS surface was developed. The other two similar pyrazolic inhibitors namely, N-(1*H*-pyrazol-1-yl)methyl)-5-bromopyridin-2-amine (**18**) and ((1*H*-pyrazol-1-yl)methylamino) benzoic acid (**19**), was also investigated in carbon steel (CS) in 1.0 M HCl using diverse methods. The estimated inhibitory power in 10^{-3} M concentration showing that compound **18** is the most effectual protector with 98% effectiveness and its efficiency against corrosion improved with concentration of pyrazole derivative. The adsorption of all the above inhibitors also follows the Langmuir isotherm [35].

Another novel inhibitor (*E*)-*N*′-(4-chlorobenzylidene)-2-(3,5-dimethyl-1*H*-pyrazol-1-yl)acetohydrazide (**21**) performed significantly better against MS corrosion in HCl solution (94% efficiency) than (*E*)-*N*′-benzylidene-2-(3,5-dimethyl-1*H*-pyrazol-1-yl)acetohydrazide (**20**) (80% efficiency) at the maximum (10^{-3} M) concentration. The thermodynamic parameters suggested chemisorption of inhibitors **20** and **21** above MS by creating a protective layer which is confirmed by the SEM analysis. Likewise, according to the polarisation measurements the anti-corrosion performance of (*E*)-2-(3,5-dimethyl-1*H*-pyrazol-1-yl)-*N*′-(4-hydroxy-3-methoxybenzylidene)acetohydrazide (**22**) and (*E*)-2-(3,5-dimethyl-1*H*-pyrazol-1-yl)-*N*′-(furan-2-ylmethylene)acetohydrazide (**23**) at 10^{-3} M was found to be 97.6% and 85.9%, respectively. Moreover, according to Tafel polarisation curves, these tested compounds exhibited mixed behaviour. It is apparent that these tested pyrazoles obey the Langmuir isotherm, furthermore, DFT, Monte Carlo and molecular dynamic (MD) simulation data pinpoint the adsorption centers of corrosion inhibitors [36,37].

Similarly, the inhibition power of new derivatives with the pyrazole moiety *viz.* 2-(3,5-dimethyl-1*H*-pyrazol-1-yl)-*N*′-(4-(dimethylamino)benzylidene)acetohydrazide (**24**), 2-(3,5-dimethyl-1*H*-pyrazol-1-yl)-*N*′-(4-methylbenzylidene)acetohydrazide (**25**) and 2-(3,5-dimethyl-1*H*-pyrazol-1-yl)-*N*′-(4-fluorobenzylidene)acetohydrazide (**26**) were also reported against deterioration of MS in 1.0 M HCl, by means of the weight loss (WL), stationary and transitional methods were investigated. The investigational outcomes demonstrate that the corrosion hindrance potentials enhanced with concentration of pyrazole derivatives and achieve 96% for compound **24** at 10^{-3} M. In terms of polarisation curves, the pyrazole derivatives were mixed type inhibitors. The model of El-Awady and Flory–Huggins assumes that the adsorption of inhibitor molecules on the steel surface occur as a result of displacing higher number of water molecules. The Temkin and Frumkin isotherm shows a strongly repulsive lateral interaction due to the negative interaction coefficient. The experimental and DFT investigations were in good agreement. The inhibition efficiency of the compounds in solution follows the order: **24** > **25** > **26** [38].

The efficiency of Schiff bases containing pyrazole moiety *viz*. *N*-(5-chloro-3-methyl-1-phenyl-1*H*-pyrazol-4-yl) methylene-naphthalen-1-amine (**27**) and *N*-(5-chloro-3-methyl-1-phenyl-1*H*-pyrazol-4-yl)methylene-4-methoxyaniline (**28**) as an anticorrosive for MS in HCl was examined *via* EIS, PDP and WL methods [39]. All these investigations showed the strong efficiency of these Schiff's bases in preventing corrosion of MS in acid medium. Inhibition efficiencies for Schiff bases **27** and **28** at 298 K, respectively, were 94.60% and 91.99%. However, their effectiveness was slightly dropped to 89.17% and 88.20% at 318 K. The electrochemical results showed that both compounds acted as mixed-kind inhibitors, leading to a consistent decrease in corrosion. The multimodal adsorption is indicated by the Gibb's free energy of adsorption. The Fukui functions and DFT analysis matched well with the experimental findings.

Two compounds, 6-amino-4-(4-methoxyphenyl)-3-methyl-2,4-dihydropyrano[2,3-*c*]pyrazole-5-carbonitrile (**29**) and 6-amino-4-(4-chlorophenyl)-3-methyl-2,4-dihydropyrano[2,3-*c*]-pyrazole-5-carbonitrile (**30**), function as inhibitors for MS corrosion in a 15% HCl solution [40]. The findings from the experiment indicated that as the inhibitor concentration rose, the inhibitory effect also increased, but this effect was reversed at higher temperatures. In acid medium at 303 K, 300 ppm concentration of compounds **29** and **30** achieved corrosion inhibition efficiency of 96.1% and 94.6%, respectively. Both inhibitors were found to be of mixed type according to PDP studies and adhered to the MS surface according to the Langmuir adsorption isotherm.

Several pyrazolopyridine derivatives *viz*. 4-(2-chloro-6-flurophenyl)-3-methyl-6-oxo-4,5,6,7-tetrahydro-2*H*-pyrazolo-[3,4-*b*] pyridine-5-carbonitrile (**31**), 3-methyl-6-oxo-4,5,6,7-tetrahydro-2*H*-pyrazolo[3,4-*b*]pyridine-5-carbonitrile (**32**), 3-methyl-6-oxo-4-(*p*-tolyl)-4,5,6,7-tetrahydro-2*H*-pyrazolo-[3,4-*b*] pyridine-5-carbonitrile (**33**), 4-(4-methoxyphenyl)-3-methyl-6-oxo-4,5,6,7-tetrahydro-2*H*-pyrazolo[3,4-*b*]pyridine-5-carbonitrile (**34**) and 3-methyl-6-oxo-4-(3,4,5-trimethoxyphenyl)-4,5,6,7-tetrahydro-2*H*-pyrazolo[3,4-*b*]pyridine-5-carbonitrile (**35**) also exhibit corrosion mitigation on the MS in HCl acid medium [41]. The PDP records designated that all these pyrazolo[3,4-*b*]pyridine derivatives displayed a mixed type inhibition with cathodic predominance. Compound **35** shows a significant anticorrosion efficiency of 95.2% when tested at 100 ppm concentration. It is also evident from the

analysis of adsorption isotherms that all these compounds follow the Langmuir isotherm.

Similarly, novel pyrazole derivatives bearing carbonitrile *viz.* 6′-amino-3′-methyl-2-oxo-1′*H*-spiro[indoline-3,4′-pyrano-[2,3-*c*]pyrazole]-5′-carbonitrile (**36**) and 6′-amino-3′-methyl-2-oxo-1′-phenyl-1′*H*-spiro[indoline-3,4′-pyrano[2,3-*c*]pyrazole]-5′-carbonitrile (**37**) also exhibited the effective corrosion miti-gation on MS in 1.0 M HCl medium [42]. However, **37** exhibit higher inhibition efficiency of 96.95% whereas the inhibitor **36** exhibit 95.65% inhibition efficiency. The electrochemical studies showed that the both compounds act as mixed-type inhibitors. DFT and MD results confirmed strong adsorption on the mild steel surface in a parallel orientation, enhancing surface protection. The adsorption data best fit the Langmuir isotherm, with a regression coefficient close to one.

A benzothiazole-linked pyrazole derivative compound **38** was synthesised and its capability to hinder corrosion of carbon steel (CS) immersed in HCl (1.0 Mol/L) solution was reported by Maia *et al*. [43]. The experimental outcomes exposed that the inhibitor **38** was concentration dependent and achieved its maximum efficiency (93%) at 600 mg L^{-1}. Based on the quantum chemical calculations, it has been proven that inhibitor **38** has the ability to interact with the surface of the metal. Therefore, theoretical and experimental consequences concur that the inhibitor **38** has an ability to restrict corrosion effectively. Another type of pyrazole derivative containing pyridine and acetohydrazide-based pyrazoline moieties, namely 1-[5-(4-bromophenyl)-3-(6-methoxypyridine-3-yl)-4,5-dihydro-1*H*-pyrazol-1-yl]ethane-1-one (**39**) was also estimated as anti-corrosive agents to protect MS from HCl environment [44]. The anti-corrosion activity was observed to increases with increasing inhibitor concentration, but decrease with the increased temperatures. A maximum corrosion inhibition efficiency of 91.1% was obtained at an inhibitor concentration of 40 ppm at 303 K. Surface analysis confirmed the formation of a protective inhibitor film on the mild steel surface, effectively suppressing metal dissolution. The electrochemical measurements supported this behaviour, while the comparative evaluation with related compounds highlighted the multifunctional potential of the inhibitor.

Novel pyranopyrazole derivatives such as ethyl 6-amino-3-methyl-4-(3-nitrophenyl)-2,4-dihydro-pyrano[2,3-*c*]pyrazole-5-carboxylate (**40**), ethyl 6-amino-3-methyl-4(phenyl)-2,4-dihydropyrano[2,3-*c*]pyrazole-5-carboxylate (**41**) and ethyl 6-amino-3-methyl-4-(*p*-tolyl)-2,4-dihydropyrano[2,3-*c*]pyrazole-5-carboxylate (**42**) were also performed as a inhibitors for corrosion of MS exposed in 1.0 M HCl environment [45]. Of the three inhibitors, compound **42** exhibited the highest efficiency of 98.8% at 100 mg/L. The potentiodynamic polarization analysis revealed that the pyranopyrazole derivatives function as mixed-type inhibitors with dominant cathodic control. The electrochemical results showed strong agreement with DFT calculations, while Fukui function analysis identified the principal electrophilic and nucleophilic reactive centers. Molecular dynamics simulations further demonstrated stable, near-parallel adsorption of the inhibitor molecules on the metal surface with high binding energies, confirming their strong surface affinity. The order of adsorption stability decreases as follows: **42** > **41** > **40**, based on the observed inhibition efficiency in experiments. The MD simulations and quantum chemical results revealed that the inhibitors exhibit higher adsorption over the MS surface in an aqueous environment compared to a vacuum environment.

Two novel aryl pyrazole derivatives containing benzoyloxy group *viz*. methyl 5-(4-chlorobenzoyloxy)-1-phenyl-1*H*-pyrazole-3-carboxylate (**43**) and another methoxyphenyl group *viz.* 5-(4-methoxyphenyl)-3-(4-methylphenyl)-4,5-dihydro-1*H*-pyrazol-1-yl-(pyridin-4-yl)methanone (**44**) were also found to be effective as anti-corrosive agent for the protection of MS immersed in HCl (15%) medium [46]. The corrosion hindrance efficiency was found to be 92.0% and 95.9%, for the inhibitors **43** and **44** at the concentration of 250 ppm, respectively. The PDP curves revealed that both the compounds operate as a mixed-kind corrosion defender. Both inhibitors observed to follow the Langmuir model adsorption isotherm and the quantum chemical calculations of these inhibitors confirmed elevated E_{HOMO}, lower E_{LUMO} values and lesser ΔE value, demonstrating that both studied compounds are excellent inhibitor for MS in HCl solution.

Three Schiff surfactants with pyrazole moiety, for example, *N*,*N*-dimethyl-4-(((1-methyl-2-phenyl-2,3-dihydro-1*H*-pyrazol-4-yl)imino)methyl)-*N*-octylbenzenaminium bromide (**45**) *N*,*N*-dimethyl-4-(((1-methyl-2-phenyl-2,3-dihydro-1*H*-pyrazol-4-yl)imino)methyl)-*N*-dodecyl benzenaminium bromide (**46**) and *N*,*N*-dimethyl-4-(((1-methyl-2-phenyl-2,3-dihydro-1*H*-pyrazol-4-yl)imino)methyl)-*N*-hexadecylbenzenaminium bromide (**47**) were synthesized and its anticorrosion efficiency against deterioration of CS in 1.0 M HCl medium was investigated. Adsorption of these surfactants on CS follows the Langmuir isotherm. All these inhibitors absorbed on CS *via* chemisorption mechanism were confirmed through standard free energy values. The EIS curves confirm the mixed-kind performance with the protection efficiencies of 86.48%, 94.00% and 95.65% in 5×10^{-3} M concentration of inhibitors **45**, **46** and **47**, respectively. From the experimental outcomes, it was accomplished that the length of hydrocarbon chain of the inhibitor molecule responsible for increase in protective efficiency [47].

The effectiveness of other novel pyrazole based Schiff base corrosion inhibitor containing benzylidene group, *e.g.*, (3,5-dimethyl-1*H*-pyrazol-1-yl)(4-((3,4-dimethoxybenzylidene)-amino)phenyl)methanone (**48**), 3,5-dimethyl-1*H*-pyrazol-1-yl)-(4-((4-hydroxybenzylidene)amino)phenyl)methanone (**49**) and (3,5-dimethyl-1*H*-pyrazol-1-yl)(4-((4-chlorobenzylidene)-amino)phenyl)methanone) (**50**) was tested on CS in 1.0 M HCl *via* electrochemical and chemical investigations [48-50]. It was found that the effectiveness of inhibition increased as the temperature increased. Inhibition efficiencies reached a maximum of 95.5% for **48** at higher temperatures and inhibitor concentrations and 89.5% for **49**. An inhibition efficiency of 89.5% was reached with inhibitor **50** at 400 ppm and 60 ºC as the optimal conditions. Corrosion protection resulted from spontaneous Langmuir-type adsorption of the inhibitors on the metal surface. The electrochemical and surface analyses confirmed mixed-type behaviour and protective film formation, supported by DFT insights into structure-activity relationships.

The anticorrosion performance of synthesized pyrazole carbohydrazide derivatives *viz*. (*E*)-5-amino-3-(4-methoxy-

phenyl)-*N*′-(1-(4-methoxyphenyl)ethylidene)-1*H*-pyrazole-4-carbohydrazide (**51**) and (*E*)-5-amino-*N*′-(4-chlorobenzylidene)-3-(4-chlorophenyl)-1*H*-pyrazole-4-carbohydrazide (**52**) on MS in 15% HCl was investigated by Paul *et al*. [51]. The inhibitor **51** and **52** at 300 ppm displayed 98.26% and 96.21% anti-corrosion efficiencies, respectively at ambient temperature. The development of defensive coats of protectors on MS plane was proved by AFM and FESEM images. According to thermodynamic results, both inhibitors **51** and **52** exhibited mixed type adsorption.

Laadam *et al*. [52] investigated the influence of corrosion inhibition using novel heteroaryl-substituted pyrazole ester compound *viz*. ethyl 5-methyl-1-(((6-methyl-4-nitro-pyridin-3-yl)amino)methyl)-1*H*-pyrazole-3-carboxylate (**53**) on CS in 1.0 M HCl medium. The experimental findings demonstrated that as the inhibitor concentration rose, the inhibition effectiveness of **53** increased up to 92% at 303 K with a 10^{-3} M concentration, but decreased as temperature rose. PDP results indicate anodic behaviour, while Nyquist plots reveal higher polarisation resistance with increasing **53** concentrations due to inhibitor molecule adsorption on the CS. The adsorption of inhibitor **53** on CS followed the Langmuir isotherm. The mechanism of the inhibition process was predicted based on the quantum chemical calculations.

The prevention of MS from HCl corrosion by novel pyrazole-pyridine-amine hybrids compounds namely, 5-bromo-*N*-((3,5-dimethyl-1*H*-pyrazol-1-yl)pyridine-2-amine (**54**) and 3,5-dibromo-*N*-((3,5-dimethyl-1*H*-pyrazol-1-yl)pyridine-2-amine (**55**) as corrosion inhibitors was investigated by Touzani *et al*. [53]. Based on the experimental studies, the inhibition efficiency increased with increasing inhibitor concentration, reaching 95% for compound 55 at 10^{-3} M. Potentiodynamic polarization studies indicated the mixed-type inhibition, suppressing both hydrogen evolution and iron dissolution. The adsorption followed the Langmuir isotherm model and theoretical analyses showed good agreement with experimental findings. The novel hybrids of pyrazalone-sulfonamides, 4-(2-(3-methyl-5-oxo-1-phenyl-1*H*-pyrazol-4(5*H*)-ylidene)-hydrazinyl)-*N*-(thiazol-2-yl)benzenesulonamide (**56**) and *N*-(4,6-dimethylpyrimidin-2-yl)-4-(2-(3-methyl-5-oxo-1-phenyl-1*H*-pyrazol-4(5*H*)-ylidene)hydrazinyl)benzenesulfonamide (**57**), were also investigated as MS inhibitors from corrosion of 1.0 M HCl medium at 298 K to 323 K by means of the chemical and electrochemical calculations [54]. Both compounds followed the Langmuir adsorption isotherm model. The SEM and EDX analyses confirmed the formation of a protective inhibitor film on the metal surface. At 500 ppm, compounds 56 and 57 exhibited inhibition efficiencies of 95.17% and 94.02%, respectively, and acted as mixed-type inhibitors.

The corrosion inhibition performance of simple monocyclic pyrazole, 3-phenyl-1*H*-pyrazole-4-carboxaldehyde (**58**) [55] and the fused bicyclic pyrazolopyrimidine derivative, 1,5-diallyl-1H-pyrazolo[3,4-d]pyrimidin-4(5H)-one (**59**) [56], was investigated on mild steel in 1.0 M HCl solution. The polarisation data specified that these inhibitors act as mixed kind protector and thermodynamic parameters shown that this molecule obeys Langmuir adsorption isotherm. The level of inhibition effectiveness is influenced by the concentration of inhibitor present, with a maximum of 96.33% for **58** and 94% for **59**. The examination with a micrographic analysis showed that there is a barrier layer present on the surface of the electrode, which is responsible for the protection of MS from deterioration. The theoretical findings aligned with the experimental outcomes [55,56].

Tebbji *et al*. [57] synthesised closely related pyrazole derivatives differing in the oxidation state at the C3 position and investigated the corrosion inhibition behaviour of 5-methyl-1-(pyridin-2-yl)-1*H*-pyrazole-3-carboxylate (**60**) and (5-methyl-1-(pyridin-2-yl)-1*H*-pyrazol-3-yl)methanol (**61**) on mild steel in 1.0 M HCl at 308 K using chemical and electrochemical methods. Inhibition efficiency increased with concentration, reaching 94% for compound **61** at 10^{-3} M. The polarization studies showed that both compounds act mainly as cathodic inhibitors without affecting the hydrogen evolution mechanism and their adsorption followed the Frumkin isotherm model.

Punitha *et al*. [19,22] also synthesized pyrazole derivatives with substitution at C3 and C5, 1*H*-pyrazole-3,5-dicarboxylic acid 5-benzyl ester 3-phenyl ester (**62**) and 5-acetyl-2*H*-pyrazole-3-carboxylic acid ethyl ester (**63**), respectively exposed fine anticorrosion efficiency against MS corrosion. Interactions of these inhibitors **62** and **63** with the MS plane submerged in 1.0 M HCl solution have been inspected systematically by utilizing WL, PDP and EIS measurements. The inhibitory process of both the studied inhibitor molecules follows the Langmuir model of adsorption isotherm. These molecules successfully reduce the oxidation of the metal with utmost efficiency of 91.55% and 90.75%, respectively for **62** and **63**. The PDP studies confirmed that these inhibitors predominately control the anodic reaction. All the thermodynamic parameters conclude the both chemisorption and physisorption.

Motawea & Abdelaziz [58] synthesized two newly organic corrosion inhibitors containing pyrazole moieties having -CN and -COC_2H_5 substitutents at C-3 position, namely 2,4-diamino-5-(5-amino-3-hydroxy-1*H*-pyrazole-1-carbonyl)thiophene-3-carbonitrile (**64**) and 1-(2,4-diamino-5-(5-amino-3-hydroxy-1*H*-pyrazole-1-carbonyl)thiophen-3-yl)propan-1-one (**65**) were assessed as an anticorrosive agents for the protection of carbon steel in 1.0 M HCl. The conductometric and spectrophotometric methods were employed to explore the potential of chemisorption between the carbon steel plane and the inhibitors studied. The highest inhibition efficiencies of 94.00% for derivatives **64** and 95.00% for **65** in 5×10^{-4} M concentration reached after one day immersion period at 333 K. Similarly, 5-chloro-1-phenyl-3-methyl pyrazolo-4-methine-thiosemicarbazone (**66**) was also investigated as CS inhibitor in HCl medium by chemical and electrochemical methods [59]. The corrosion rate decreases with raising the concentration of **66** and temperature. The PDP information specified that **66** behaved as mixed kind inhibitor, but under prominent cathodic control. SEM morphology confirms the formation of passive layer on the carbon steel surface.

Two green pyrazole molecules, *N*-((3,5 dimethyl-1*H*-pyrazol-1-yl)methyl)-4-nitroaniline (**67**), *N*-((1*H*-pyrazol-1-yl)-methyl)-4-nitroaniline (**68**) and ethyl 5-methyl-1-(((4-nitrophenyl)amino)methyl)-1*H*-pyrazole-3-carboxylate (**69**), were tested by Adlani *et al*. [60,61] for their performance as corrosion inhibitors for carbon steel in 1.0 M HCl medium.

Both electrochemical and chemical measurements were used in order to evaluate the inhibition efficiency of the investigated molecules. Compounds **67**, **68** and **69** displayed good corrosion inhibition efficiency, with inhibition efficiencies of 95.1%, 91.8% and 90.8% at 10^{-3} M concentration for the pyrazoles **67**, **68** and **69**, respectively. In accordance with the conclusions of PDP, all the inhibitors act as mixed-kind protectors.

Shaban *et al*. [62] synthesized two pyrazole derivatives ((4-bromophenyl)hydrazono)-3-(5′-(4-nitrophenylazo)-2′-hydroxyphenyl)-2-pyrazolin-5-one (**70**, parent pyrazolinone N-H) and ((4-bromophenyl)hydrazono)-3-(5′-(4-nitrophenylazo)-2′-hydroxyphenyl)-1-phenyl-2-pyrazolin-5-one (**71**, N-phenyl substituted analogue) as inhibitors towards carbon steel. Based on the results, compound **71** has exhibited a higher inhibition performance than compound **70** and the reason is attributed to the benzene ring acting as an active centre that impose the additional adsorption ability towards the CS. According to polarisation curves, they performed as mixed-type protectors. Structurally similar pyrazoline derivatives 4-methylphenylhydrazono-3-(2-hydroxyphenyl)-2-pyrazolin-5-one (**72**) and ((4-phenyl)hydrazono)-3-(5′-(4-nitro-phenylazo)-2′-hydroxyphenyl)-2-pyrazolin-5-one (**73**) were synthesized by Abbas *et al*. [63] in order to evaluate their corrosion inhibition behaviour on carbon steel (CS) in a 5.0 M HCl medium. The anticorrosion abilities of compounds **72** and **73** were found to enhance whenever the inhibitor concentrations were increased. Langmuir's adsorption isotherm was the finest fitted form for both the inhibitors. PDP also confirmed their mixed cathodic as well as anodic corrosion inhibition nature. The existence of nitrophenyl azo group in **73**, enhance its corrosion inhibition efficiency as compared to **72**.

Three novel hydrazone-linked pyrazolones *viz*. (*E*)-4-(2-(2-chlorophenyl)hydrazineylidene)-2-phenyl-5-(phenylamino)-2,4-dihydro-3*H*-pyrazol-3-one (**74**), (*E*)-4-(2-(2-chlorophenyl)-hydrazineylidene)-2-phenyl-2,4-dihydro-3*H*-pyrazol-3-one (**75**) and (*E*)-4-(2-(2-chlorophenyl)hydrazineylidene)-1-phenyl-pyrazolidine-3,5-dione (**76**) were investigated as effective corrosion inhibitors for stainless steel (SS) in 1.0 M HCl employing WL, EIS, PDP and EFM (electrochemical frequency modulation) methods [64]. The results showed that inhibition efficiency increased with higher concentrations of pyrazolinone derivatives and decreased with increasing temperature. Adsorption on the stainless steel (SS) surface followed the Langmuir isotherm model. Among the tested compounds, derivative **74** exhibited the highest inhibition performance in 1.0 M HCl and acted as a mixed-type inhibitor. AFM analysis further confirmed the formation of a protective adsorbed layer on the SS surface.

Corrosion inhibition efficiencies of two novel derivatives containing pyrazolylmethylamino fragment containing pyrimidine and benzoic acid *viz*. *N*-((1*H*-pyrazol-1-yl)methyl)-pyrimidin-2-amine (**77**) and 2-(((1*H*-pyrazol-1-yl)methyl)-amino)-benzoic acid (**78**), on carbon steel was evaluated in 1 M HCl medium. The results specified that the corrosion inhibition efficiency declined with temperature and rose with inhibitors concentration and reach uppermost efficiencies of 94% for **77** and 92% for **78** in 10^{-3} M concentration at 303 K, respectively. The inhibition efficiency was decreased considerably as 76.9% for **77** and 72.3% for **78** at higher temperature (333 K). PDP reports show that **78** exhibits a combination of behaviours, while **77** exhibits primarily anodic behaviour. The adsorption behaviour of the pyrazole derivatives on the carbon steel (CS) surface follows the Langmuir isotherm model. The thermodynamic parameters suggest that the inhibition process is predominantly governed by physisorption. The experimental findings were consistent with DFT calculations, while molecular dynamics simulations revealed that the inhibitors adsorb on the Fe (110) surface in both neutral and protonated forms with a near-parallel orientation [65].

Two compounds of the same category, 4-(4,5-dihydro-1*H*-pyrazol-5-yl)-*N*,*N*-dimethylaniline (**79**) and *N*,*N*-dimethyl-4-(3-methyl4,5-dihydro-1*H*-pyrazol-5-yl)aniline (**80**) (methyl substitution at C-3 of pyrazoline) have an effective corrosion obstructing capability against the MS corrosion caused by 1.0 M HCl [66,67]. The presence of a methyl group at position three resulted in a minor decrease in inhibitory effectiveness while maintaining the anticorrosive properties. The electrochemical studies show that derivatives **79** and **80** were good cathodic as well as anodic anticorrosion agent for MS in 1.0 M HCl medium. Thermodynamic study shows that the adsorption mechanism follows both chemisorption as well as physisorption. The DFT results exposed that molecule **79** (96%) is more effective than **80** (95%). The Nyquist plots show an increase in charge-transfer resistance and inhibition efficiency as the concentration of the inhibitor is increased. The pyrazole derivative **79** also restrict the oxidisation of Fe in 1.0 M HCl medium by adsorbing *via* the Langmuir isotherm protocol. In addition, all measured values of the Gibb's free energy change for adsorption show that molecules **79** and **80** were spontaneously adsorbed onto the steel surface through both physisorption and chemisorption mechanisms.

The galvanostatic cathodic polarisation performance was utilised to estimate the protection effectiveness of some substituted pyrazole derivatives (**81-89**) containing electron donating or withdrawing groups on MS dissolution in 0.5 M HCl [68]. Corrosion inhibition efficiency increased with rising concentration of pyrazole derivatives (**81-89**) until reaching a limiting value corresponding to monolayer formation on the mild steel surface. The positive shift in corrosion potential indicates predominantly anodic inhibition behaviour. At identical concentrations, methoxy-substituted derivatives (**87-89**) exhibited higher efficiency than methyl-substituted analogues (**84-86**), while bromo or cyano substitution at the 4-position reduced inhibitory performance. In several cases, the inhibition efficiencies exceeded 90%. Moreover, the adsorption followed the Langmuir isotherm model and the trends observed from Hammett constants and quantum chemical parameters showed good agreement with the electrochemical results, highlighting the influence of substituent electronic effects on inhibition performance.

The corrosion inhibition effect of new pyrazolone-aryl malononitrile conjugated derivatives namely 2-(3-amino-5-oxo-4,5-dihydro-1*H*-pyrazol-1-yl)(*p*-tolyl)methyl)malononitrile (**90**) and 2-((3-amino-5-oxo-4,5-dihydro-1*H*-pyrazol-1-yl)-(phenyl)methyl)malononitrile (**91**) on N80 steel in HCl (15%) medium has been examined using experimental, quantum chemical and surface morphological investigations [69]. The

experimental results expose that compound **90** (92% inhibition efficiency) is a better inhibitor than **91** (85.1% inhibition efficiency). Tafel polarization studies demonstrated that both pyrazolone derivatives are mixed kind protectors, however majorly suppress the cathodic corrosion. The Gibb's free energy reveals that both chemical and physical adsorption for the studied compounds **90** and **91**. Quantum chemical data confirmed that both protonated form of pyrazolone derivatives have larger adsorption and interaction capability than the neutral ones. Furthermore, MC simulations also align with the results from experiments.

A multi-substituted pyrazole aldehyde compound *viz*. 5-chloro-3-methyl-1-phenyl-1*H*-pyrazole-4-carbaldehyde (**92**) was utilised for its anti-corrosion properties for MS in HCl medium as reported by Thomas *et al.* [70]. The experimental findings demonstrate that as the inhibitor concentration rises, the inhibition effectiveness of **92** increased, but decreased as temperature and acid concentration increased. The electroanalytical test confirms a mixed-type protection of the inhibitor **92** and adsorbs over the MS by Langmuir isotherm pattern. The MD simulations designated that the inhibitor **92** interact on Fe (111) plane of the MS surface and the highest corrosion inhibition efficiency of 93.17% was attained at 100 ppm concentration. The high E_{HOMO} value assumes the larger electron donating aptitude of **92**.

The effectiveness of two new pyrazoles (new substituents 4-methoxyphenyl and *p*-tolyl at the pyrazole C-3 position) namely 2-(4-(4,5-dihydro-3-(4-methoxyphenyl)-1*H*-pyrazol-5-yl)phenoxy)acetic acid (**93**) and 2-(4-(4,5-dihydro-3-*p*-tolyl-1*H*-pyrazol-5-yl)phenoxy)acetic acid (**94**), against MS corrosion in 1.0 M HCl was investigated *via* chemical, electrochemical, SEM, XPS and computational techniques [71]. The highest anti-corrosion efficiencies of 94% and 88% at 5 mM concentration were obtained for **93** and **94**, respectively. The compounds retard the corrosion of MS at 303 K and show high inhibition efficiency at 333 K. The XPS results confirmed the physisorption and chemisorption of these inhibitors on MS plane follows Langmuir model adsorption and inhibits acid attack effectively. Electrochemical reports exposed that these new inhibitors displayed mixed-kind inhibition.

Li *et al.* [72] reported the chemical, electrochemical and quantum chemical calculations were utilised to calculate the effectiveness of corrosion inhibition of new pyrazole-triazole hybrid derivatives *viz*. 1-(3-phenyl-4,5-dihydropyrazol-1-yl)-2-(1*H*-1,2,4-triazol-1-yl)ethanone (**95**), 1-(3-(4-fluorophenyl)-4,5-dihydropyrazol-1-yl)-2-(1*H*-1,2,4-triazol-1-yl)ethanone (**96**) and 1-(3-(2,4-dichlorophenyl)-4,5-dihydropyrazol-1-yl)-2-(1*H*-1,2,4-triazol-1-yl)ethanone (**97**) on MS immersed in 1.0 M HCl solution. Inhibitor **97** possesses the maximum inhibition efficiency of 99% among the inhibitors **95**, **96** and **97**. The anti-corrosion efficiency of these inhibitors follows the order: **96** < **95** < **97**. The electrochemical analysis revealed that the inhibitors exhibit mixed-type behaviour, suppressing both anodic and cathodic reactions on mild steel. Adsorption behaviour was evaluated at different temperatures and DFT calculations identified the benzene, pyrazole, triazole and related substituents as the primary active centers responsible for surface interaction. Thermodynamic parameters indicated that the inhibition mechanism involves both physisorption and chemisorption. The adsorption process was best described by the Langmuir isotherm, suggesting monolayer coverage without significant interaction between adsorbed molecules.

The corrosion inhibition performance of the novel methyl substituted pyrazole carbohydrazide derivative, ethyl 4-(5-acetyl-4-amino-3-(thiazol-2-ylcarbamoyl)-1H-pyrazol-1-yl)-benzoate (**98**), was evaluated by Al Jahdaly & Masaret [73] on low carbon steel in 0.5 M HCl using EIS and PDP techniques. Inhibition efficiency increased with concentration, reaching approximately 89% at 303 K. Polarization studies indicated mixed-type inhibition behaviour and adsorption followed the Langmuir isotherm with contributions from both physisorption and chemisorption. Surface analyses (AFM and SEM) confirmed protective film formation, while DFT calculations identified the active adsorption sites and clarified the interaction mechanism.

Another similar structural substituted pyrazole carbohydrazide derivative *viz*. 1,5-dimethyl-1*H*-pyrazole-3-carbohydrazide (**99**) compound was also evaluated as corrosion inhibitor for mild steel in 1.0 M HCl [74]. The compound achieved 96% efficiency at 10^{-3} M, with performance increasing at higher concentrations but decreasing with temperature. The polarization results indicated mixed-type inhibition and adsorption followed the Langmuir isotherm. The surface analysis and the DFT and MC simulations also confirmed the adsorption behaviour of **99** over the metal surface.

Novel tethered pyrazole compound, (methyl-substituted pyrazole tethered *via* a methylene to benzimidazole) namely 2-[(5-methylpyrazol-3-yl)methyl]benzimidazole (**100**) has been investigated for its inhibitory potential for the protection of carbon steel in 1.0 M HCl using EIS, PDP and WL investigations at 293 K [75]. In addition, the MC simulations and DFT/B3LYP-basis set of computations were utilised as a supportive evidence to explain the adsorption behaviour of **100** on the carbon steel surface. Inhibition efficiency of compound 100 increased with concentration, reaching a maximum of 97% at 5×10^{-3} M, but decreased at higher temperatures. The adsorption followed the Langmuir isotherm and polarization curves indicated mixed-type inhibition behaviour. The protonated form of the molecule showed stronger interaction with the carbon steel surface than the neutral form, with its planar structure promoting parallel adsorption through intramolecular hydrogen bonding.

Cao *et al*. [76] investigated the effectiveness of corrosion inhibition of 1-phenyl-3-methyl-5-pyrazolone (**101**) inhibitor on MS in 1.0 M HCl was explored through WL, PDP curve, EIS, Raman spectrum and quantum chemical methods. About 93% inhibition effectiveness was achieved in the existence of 1×10^{-3} M concentration of compound **101** whereas the efficiency was decreased to 32% in 1×10^{-5} M concentration. The EIS data revealed that the inhibitor **101** excellently inhibit corrosion of MS in acidic medium and its protection efficiency reached greater than 97.2% in 1×10^{-3} M concentration at 298 K. PDP data revealed the great decrease of corrosion current in the existence of **101** in HCl medium and confirmed the mixed-type corrosion inhibition action. The quantum chemical measurement found the active adsorption locations as oxygen atom and phenyl group present in the studied inhibitor **101**. The linear regression analysis of the plot of C/θ

versus C indicates that the inhibitor adheres to the Langmuir adsorption isotherm.

The influence of aryl substituted pyrazoline-quinoxaline analogues namely 1-[3-(3-methoxyphenyl)-5-(quinoxalin-6-yl)-4,5-dihydropyrazol-1-yl]propan-1-one (**102**) and 1-(3-(4-chlorophenyl)-5-(quinoxalin-6-yl)-4,5-dihydro-1*H*-pyrazol-1-yl)propan-1-one (**103**) on corrosion inhibition propensity on MS in 1.0 M HCl solution was studied using WL, PDP, EIS and computational analysis [77]. Both inhibitors **102** and **103** effectively protected mild steel in acidic medium, with inhibition efficiency increasing with concentration. Both formed a pseudo-capacitive protective layer and exhibited mixed type inhibition behaviour. Adsorption followed the Langmuir isotherm, with compound **102** showing combined physisorption and chemisorption, whereas compound **103** predominantly underwent chemisorption. Monte Carlo simulations confirmed stable adsorption on the Fe (110) surface, and SEM analysis verified protective film formation. DFT results indicated superior inhibition performance for compound **102**, attributed to its stronger electron-donating ability, while the protonated form of compound **103** demonstrated enhanced inhibition compared to its neutral form.

Corrosion inhibition behaviour of *bis*-pyrazole derivatives: Arrousse *et al.* [78] investigated *bis*-pyrazolylmethyl amino derivative 2-(*bis*((1*H*-pyrazol-1-yl)methyl)amino)pyrimidine-4,6-diol (**104**) as anticorrosive agent for MS in HCl environment with 88% inhibition efficiency. A comparative evaluation of inhibitors **9** and **104** demonstrated superior corrosion protection by compound **104** on mild steel in HCl, attributed to the presence of two pyrazole moieties that enhance coordination with the metal surface. Tafel polarization results indicated mixed-type inhibition behaviour for both compounds. Their adsorption on mild steel followed the El Awady adsorption isotherm model.

Kaddouri *et al.* [79] reported the synthesis and corrosion behaviour of *p*-benzonitrile-*bis*-pyrazolylmethyl analogues namely 4-(*bis*((1H-pyrazol-1-yl)methyl)amino)benzonitrile (**105**) and 4-(*bis*((3,5-dimethyl-1*H*-pyrazol-1-yl)methyl)amino)benzonitrile (**106**). Both compounds demonstrated excellent inhibition of mild steel in acidic medium, achieving inhibition efficiencies of 92.3% and 92.4%, respectively, at a concentration of 10^{-3} M, as determined by weight loss and electrochemical measurements. The slightly superior performance of compound **106** is associated with the electron-releasing methyl substituents on the pyrazole rings. These groups enhance the electron density at the nitrogen donor sites, promoting stronger interaction with the metal surface through coordination bonding. In acidic solution, protonation of the heterocyclic nitrogen atoms further facilitates adsorption, leading to the formation of a protective film over the mild steel surface. Adsorption of both inhibitors follows the Langmuir isotherm indicating monolayer coverage with uniform adsorption sites. Thermodynamic parameters and electrochemical impedance data suggest that the inhibition mechanism involves a combined physisorption-chemisorption process. Density functional theory (DFT) calculations support these findings by confirming favourable electronic properties and strong adsorption tendencies for the methyl-substituted analogue.

Verma *et al.* [80] synthesised homologous series of arylmethylene-bridged *bis*-pyrazolone derivatives and the investigated the corrosion inhibition efficiencies of *bis* pyrazole inhibitors, 4,4′-(phenylmethylene)*bis*(3-methyl-1-phenyl-1*H*-pyrazol-5-ol) (**107**), 4,4′-((4-nitrophenyl)methylene)*bis*(3-methyl-1-phenyl-1*H*-pyrazol-5-ol) (**108**), 4,4′-((4-hydroxyphenyl) methylene)*bis*(3-methyl-1-phenyl-1*H*-pyrazol-5-ol) (**109**) and 4,4′-((2-hydroxy-4-methoxyphenyl)methylene-*bis*-(3-methyl-1-phenyl-1*H*-pyrazol-5-ol) (**110**) are 89.77%, 90.90%, 91.47% and 94.88% on MS in acidic environment. All the compounds follow the Langmuir model with best regression coefficient ($R^2 \approx 1$) values. The inhibitor was classified as mixed type due to the electrode potential shift being less than -85 mV in PDP data. Pyrazoles containing an electron donating substituent exhibited a higher level of inhibition than those with an electron withdrawing substituent.

Using chemical as well as electrochemical techniques, the inhibition efficiencies of novel homologous series of *N*,*N*-*bis*(pyrazolylmethyl) tertiary amines *viz.* *N*,*N*-*bis*(3,5-dimethyl-pyrazol-1-ylmethyl)cyclohexylamine (**111**), *N*,*N*-*bis*(3,5-dimethyl-pyrazol-1-ylmethyl)ethanolamine (**112**), *N*,*N*-*bis*-(3,5-dimethylpyrazol-1-ylmethyl)allylamine (**113**), *N*,*N*-*bis*(3-carboethoxy-5-methylpyrazol-1-ylmethyl)cyclohexylamine (**114**), *N*-benzyl-*N*,*N*-*bis*[(3,5-dimethyl-1*H*-pyrazol-1-yl)methyl]amine (**115**), *N*,*N*-*bis*[(3,5-dimethyl-1*H*-pyrazol-1-yl)methyl]-N4,N4-dimethyl-1,4-benzenediamine (**116**) and *N*,*N*-*bis*[(3,5-dimethyl-1*H*-pyrazol-1-yl)methyl]aniline (**117**) against the corrosion of MS by 1.0 M HCl solution have been reported. The experimental finding reveals that the highest inhibition percentage of 96% was reached for the compound **117**. The polarisation curves indicate the mixed behaviour of bipyrazolic compounds. Thus, they suppress both cathodic and anodic oxidisation of MS working electrode. For compounds **111** and **114**, anticorrosion efficiency raised with rising the temperature, whereas for compounds **112**, **113, 115**, **116** and **117** it decreased. The compound **114** has lower inhibition effectiveness due to the inductive effect of ester group, which diminishes electronic density on N at α-position, along with the steric effect of this group [81-83].

The inhibitive efficiencies of isomers of *bis*(pyrazolylmethyl)aminophenol such as 4-{*bis*[(1,5-dimethyl-1*H*-pyrazol-yl-3-yl)methyl]amino}phenol (**118**) and 4-{*bis*[(3,5-dimethyl-1*H*-pyrazolyl-1-yl)methyl]amino}phenol (**119**), on mild steel corrosion in 1.0 M HCl solution was examined at 308 K using weight loss and electrochemical techniques. The inhibition efficiencies determined from these methods show good correlation. The polarisation curves show that all these bipyrazolic derivatives function as inhibitors of both cathodic and anodic corrosion (mixed-type). This PDP studies showed that both compounds are effective inhibitors, with almost 95% effi-ciency at a concentration of 5×10^{-4} M. Among these isomers, compound **118** has higher anticorrosion efficiency compared to **119**. Steel corrosion in 1.0 M HCl without or with bipyrazolic compounds at 5×10^{-4} M in the temperature range of 308 to 353 K was determined to calculate the activation parameters. The isomers adhere to the steel surface based on a Temkin isotherm model [84].

The relation between the inhibition efficiencies of new homologous bis(pyrazolylmethyl) tertiary amines, *N*,*N*-*bis*-

(3,5-dimethylpyrazol-1-ylmethyl)cyclohexylamine (**120**), *N*,*N*-*bis*(3,5-dimethylpyrazol-1-ylmethyl)ethanolamine (**121**), *N*,*N*-*bis*(3,5-dimethylpyrazol-1-ylmethyl)allylamine (**122**) and *N*,*N*-*bis*(3-carboethoxy-5-methylpyrazol-1-ylmethyl)cyclohexylamine (**123**), on corrosion of MS by HCl was explained *via* DFT using B3LYP/6-31G(d) level. These bipyrazole compounds displayed the high protection capabilities against deterioration of MS immersed in acidic medium. The designed quantum chemical data used to correlate the anticorrosion efficiency of studied inhibitors. The probability to contribute electrons to the empty orbitals is confirmed by high E_{HOMO} values. The highest corrosion hindrance efficiency of compounds **120**, **121** and **122** were due to the increasing E_{HOMO} values and the decreasing E_{LUMO} values. This concept was in an excellent conformity with the experimental findings. The lower total energy for the inhibitor **123** revealed the weaker corrosion inhibition tendency, whereas the higher total energy (-859.15 kcal mol^{-1}) for the derivative **122** proves the higher inhibition. This high inhibition for the inhibitor **122** was also correlated with the low electronegativity [85].

Selatnia *et al*. [86] investigated the anticorrosion efficiency of a novel *bis*-pyrazoline molecule *viz*. 5,5′-(1,4-phenylene)*bis*[1-formyl-4,5-dihydro-3-phenyl-1*H*-pyrazole] (**124**) on carbon steel in 1.0 M HCl using WL, PDP and EIS techniques. The anticorrosion efficiency of **124** was increased up to 91% with enhances its concentration to 400 ppm. By affecting both anodic and cathodic corrosion reactions, the inhibitor **124** acts as a mixed kind protector. Both physical and chemical adsorptions of **124** on carbon steel surface follows Langmuir mode of isotherm spontaneously. The surface morphological investigation confirmed the development of inhibitor film. The large negative interaction energy value of MD confirms the well-built interaction among the inhibitor and carbon steel surface.

Bendaha *et al*. [87] reported the adsorption and corrosion inhibition studies on mild steel (MS) in HCl solution using *bis*(pyrazolylmethyl)amino-alcohol derivatives, for example, 1-[*bis*-(3-carbomethoxy-5-methyl-pyrazol-1-ylmethyl)amino]-propan-2-ol (**125**) and 3-[*bis*-(3,5-dimethyl-pyrazol-1-ylmethyl)amino]propan-1-ol (**126**) in the temperature range of 308-323 K. Compound **125** showed better corrosion inhibition than compound **126**, with efficiencies of 92% and 87%, respectively, for mild steel in acidic solution. The inhibition efficiency increased with increasing inhibitor concentration, indicating improved surface coverage, while it decreased at higher temperatures, suggesting partial desorption. Similarly, Elayyachy *et al*. [88] studied the inhibition effect of *N*,*N*′-*bis* (3,5-dimethylpyrazol-1-ylmethyl)-pentan-1-ol-amine (**127**) on steel in 1.0 M HCl at 308 K using weight loss and polarization techniques and achieved about 82% efficiency. Its adsorption obeyed the Langmuir isotherm, indicating monolayer formation. Polarization results showed hydrogen evolution was activation-controlled, with inhibition mainly due to surface adsorption and possible complex formation on the steel surface.

Compounds **128-131** containing *bis*-pyrazole framework have established into more structurally diverse systems, ranging from rigid conjugated hydrazone-linked architectures (**128**) to flexible amino acid derivatives (**129**) and tetradentate diamine-based ligands (**130-131**), enabling systematic investigation of rigidity, electronic substitution, denticity and coordination behaviour. The water-soluble 4,4-([1,1′-biphenyl]-4,4-diyl*bis*(hydrazin-2-yl-1-ylidene))*bis*(5-(2-hydroxyphenyl)-2,4-dihydro-3*H*-pyrazol-3-one) (**128**) exhibited 93.3% inhibition efficiency for mild steel in 1.0 M HCl [89], following the Langmuir isotherm and acting as a mixed-type inhibitor. Furthermore, theoretical calculations were executed to recognize the active sites on inhibitor **128** to facilitate adsorption and the surface protection.

Compound 11-(*bis*((1*H*-pyrazol-1-yl)methyl)amino)undecanoic acid (**129**) showed concentration-dependent inhibition, reaching 99.5% efficiency at 10^{-3} M. Tafel analysis confirmed mixed-type behaviour with dominant anodic control. Langmuir adsorption and high binding energy values (398, 340 eV) indicated strong chemisorption on the Fe surface [90]. Bouklah *et al*. [91] synthesised *N*,*N*′-*bis*[(3-ethylcarboxylate-5-methyl-1*H*-pyrazol-1-yl)methyl]-*N*,*N*′-dimethyl ethane-1,2-diamine (**130**) and *N*,*N*′-*bis*-[(3,5-dimethyl-1*H*-pyrazol-1-yl)-methyl]-*N*,*N*′-dimethylethane-1,2-diamine (**131**) and acted as mixed-type inhibitors in 1.0 M HCl, with efficiencies of 95.5% and 87%, respectively. DFT calculations exhibit strong correlations with the experimental results and it is evident that corrosion mitigation effectiveness raises in the order: **130** > **131**.

Compounds **132-136** represent diverse derivatives of the *bis*(pyrazolylmethyl) ligand family, incorporating rigid aromatic (pyridine), flexible aliphatic (amino acid-type) and cyclic diamine (piperazine) backbones with tunable electronic substitutions, enabling systematic control over denticity, rigidity, coordination strength and potential metal-binding geometry.

Compound, 1,1′-(pyridine-2,6-dihyl*bis*(methylene))-*bis*-(5-methyl-1-*H*-pyrazole-3-carboxylic acid) (**132**) was evaluated for mild steel corrosion in 1.0 M HCl and showed 96% efficiency at 10^{-3} M based on the polarization studies [92]. Its performance improved with concentration and followed the Langmuir adsorption isotherm, indicating spontaneous monolayer adsorption. Electrochemical data confirmed mixed type inhibition without altering the hydrogen evolution mechanism.

Compounds **133** and **134**, two dimethyl-pyrazole-based amino acids *viz*. 2-[*bis*-(3,5-dimethyl-pyrazol-1-ylmethyl)-amino]-3-hydroxybutyric acid and 2-[*bis*-(3,5-dimethyl-pyrazol-1-ylmethyl)amino]pentanedioic acid, were also tested in 1.0 M HCl. At 10^{-3} M, they achieved 95.9% and 98.1% inhibition efficiency, respectively. Their action was attributed to the adsorption following the Langmuir model. The polarization and impedance results revealed mixed-type behaviour, increased charge transfer resistance with concentration and reduced efficiency at elevated temperatures [93,94].

Similarly, piperazine-linked bipyrazoles, *N*,*N*′-*bis*[(3,5-dimethyl-1*H*-pyrazol-1-yl)methyl]piperazine (**135**) and *N*,*N*′-*bis*[(3-ethylcarboxylate-5-methyl-1*H*-pyrazol-1-yl)methyl]-piperazine (**136**) [95] demonstrated inhibition efficiencies of 91% and 92% in 1.0 M HCl. A decrease in double-layer capacitance and activation energy suggested strong chemisorption involving electron sharing between iron and pyrazole nitrogen atoms.

Compounds **137-147**, trimethyl-substituted bipyrazole derivatives differing in their structural connectivity, particu-

larly in the 3,3′ and 1,3′-linkage pattern, were also systematically evaluated as corrosion inhibitors for mild steel in acidic media, where their performance was correlated with molecular structure and adsorption characteristics.

Isomer **137**, 2-(1′,5,5′-trimethyl-1*H*,1′*H*-3,3′-bipyrazol-1-yl)ethanol, showed superior performance, reaching 93% inhibition efficiency at 10^{-3} M as compared to 2-(1′,5,5′-trimethyl-1*H*,2′*H*-3,3′-bipyrazol-2-yl)ethanol (138) [96]. It was found that efficiency increased with concentration and both compounds mainly suppressed the cathodic reaction. Their adsorption followed the Langmuir isotherm and occurred spontaneously. The other related bipyrazoles like 1,5,5′-trimethyl-1*H*,2′*H*-3,3′-bipyrazole (**139**), ethyl 1′,5,5′-trimethyl-1′*H*-1,3′-bipyrazole-3-carboxylate (**140**) and (1′,5,5′-trimethyl-1′*H*-1,3′-bipyrazolyl-3-yl)methanol (**141**) were also assessed in 1.0 M HCl using electrochemical and gravimetric methods [97]. Among them, compound **139** exhibited the highest efficiency (79% at 10^{-3} M). Its adsorption fitted an S-shaped Frumkin isotherm and inhibition efficiency improved with increasing temperature. Polarization data indicated predominant cathodic inhibition behaviour.

Similarly, 3,5,5′-trimethyl-1′H-1,3′-bipyrazole (**143**) and ethyl-5,5′-dimethyl-1′H-1,3′-bipyrazole-3-carboxylate (**144**) were evaluated as corrosion inhibitors for steel in 1.0 M HCl at 308 K [98]. Compound **143** exhibited superior performance, achieving 84% efficiency at 10^{-3} M and acting predominantly as a cathodic-type inhibitor. Results from all techniques were consistent, and adsorption followed the Langmuir isotherm. Likewise, Zarrok *et al*. [99,100] synthesized and tested ethyl-5,5′-dimethyl-1′H-1,3′-bipyrazole-4-carboxylate (**145**), 1,1′,5,5′-tetramethyl-1H,1′H-3,3′-bipyrazole (**146**) and 3-(bromomethyl)-5,5′-dimethyl-1′H-1,3′-bipyrazole (**147**) were tested the inhibition efficiency on C38 steel in acidic medium. The inhibition performance followed the order: **145** < **147** < **146**, indicating that compound **146** exhibited the highest protective efficiency among the three derivatives. Thermodynamic parameters and Langmuir adsorption behaviour suggested chemisorption as the dominant mechanism. Electrochemical studies confirmed the mixed-type inhibition, with increased charge transfer resistance and reduced double-layer capacitance indicating effective surface protection.

Benabdellah *et al*. [101] synthesized a new series of substituted 3,3′-bipyrazoles bearing bulky substituent groups (**148-150**) and investigated their corrosion inhibition performance for mild steel in HCl solution. All methods showed that inhibition efficiency increased with increasing inhibitor concentration. The protective performance was strongly influenced by the substituent on the bipyrazole framework. Among the tested compounds, the chloro-substituted derivative (**150**) exhibited the highest efficiency, reaching 98% at 10^{-3} M. Polarization data indicated predominantly cathodic inhibition behaviour. Adsorption of these inhibitors on the steel surface followed the Langmuir isotherm and thermodynamic parameters supported a spontaneous adsorption process.

Touhami *et al*. [102,103] synthesized a series of *bis*-(pyrazolyl)alkanes with variable chain lengths and different substitution (**151-156**) and evaluated as corrosion inhibitors for Armco iron in 1.0 M HCl solution. Among the evaluated compounds, compound **152** exhibited the highest inhibition efficiency (93%). Its adsorption on Armco iron followed the Langmuir isotherm, whereas compound **156** showed an S-shaped adsorption profile consistent with the Frumkin model, achieving nearly 90% inhibition. The inhibition efficiency increased with temperature (308-338 K), indicating enhanced interaction with the metal surface at elevated temperatures. Polarization studies revealed that compounds **154** and **155** behaved mainly as cathodic inhibitors, while compounds **152** and **156** displayed mixed-type characteristics. The presence of two oxygen atoms in compounds **154** and **155** was associated with lower efficiencies (69% and 54%, respectively). Thus, the inhibitors bearing longer alkyl chains demonstrated comparatively reduced corrosion protection performance.

El-Ouali *et al*. [104] synthesized *bis*(pyrazolyl)alkane derivatives with reactive chloromethyl or ester (**157-159**) *viz*. 1,1′-propane-1,3-diyl*bis*[3-(chloromethyl)-5-methyl-1*H*-pyrazole] (**157**), dimethyl 1,1′-butane-1,4-diyl*bis*(5-methyl-1*H*-pyrazole-3-carboxylate) (**158**) and 1,1′-butane-1,4-diyl*bis*[3-(chloromethyl)-5-methyl-1*H*-pyrazole] (**159**) as a corrosion inhibitors and investigated its efficiency on the C38 steel in HCl medium. The weight loss and electrochemical analyses revealed that all the pyrazoles achieved over 90% corrosion inhibition efficiency, with compound **159** showing the highest performance at 96%. The PDP investigations suggested that all are predominantly inhibit the cathodic corrosion. The theoretical analysis validates the findings obtained from the chemical and electrochemical approaches.

Cherrak *et al*. [105,106] synthesized newly *bis*(pyrazole-carbohydrazide) derivatives (**160-163**) as anticorrosive inhibitors namely, *N*,*N*-*bis* (3-carbohydrazide-5-methylpyrazol-1-yl)methylene (**160**), 1,4-*bis*(3-carbohydrazide-5-methylpyrazol-1-yl)butane (**161**), 1,1′-(propane-1,3-diyl)*bis*(5-methyl-1*H*-pyrazole-3-carbohydrazide) (**162**) and 1,1′-(oxy *bis*(ethane-2,1-diyl))*bis*(5-methyl-1*H*-pyrazole-3-carbohydrazide) (**163**). The compounds were tested against deterioration of MS in 1.0 M HCl solution. At its higher concentration of 10^{-3} M, inhibitor **160** and **161** showed 98.6% and 87.8% inhibition efficiencies, respectively. Similarly, the corrosion inhibition efficiencies of **162** is 95% and **163** is 84%. The PDP experiments indicated that they inhibited corrosion in a mixed-kind fashion and obeying the Langmuir's model isotherm. As a result of the Gibb's free energy of adsorption values, the physico-chemical methods of adsorption were confirmed.

In continuation of his work, El Arrouji *et al*. [107] synthesized novel pyrazole derivative, diethyl 1,1′-(((4-acetylphenyl)azanediyl)*bis*(methylene))*bis*(5-methyl-1*H*-pyrazole-3-carboxylate) (**164**), consisting a rigid aromatic core with flexible pyrazole ester arms, on MS in 1.0 M HCl solution was investigated using WL, EIS and PDP methods. The results of the experiment showed that the effectiveness of these inhibitors in shielding increased as the inhibitor concentration rose. It shows 84% inhibition efficiency in 10^{-3} M at 308 K. The inhibitors adsorbed on the mild steel surface according to the Langmuir isotherm, forming a protective chemisorbed layer, as confirmed by SEM-EDX analysis showing a shielding film on the metal surface.

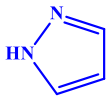

1

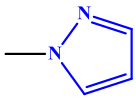

2

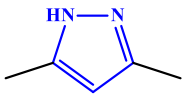

3

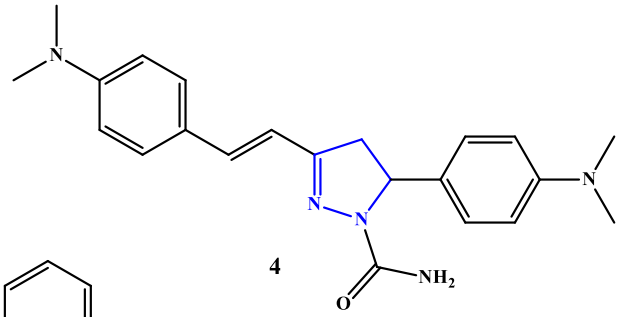

4

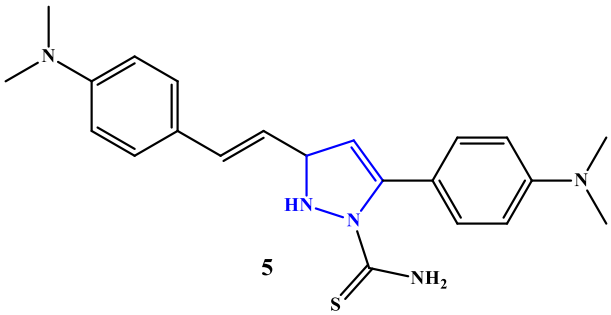

5

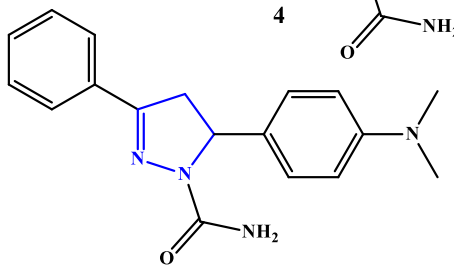

6

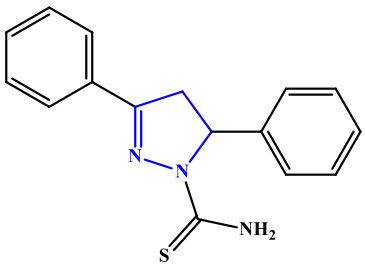

7

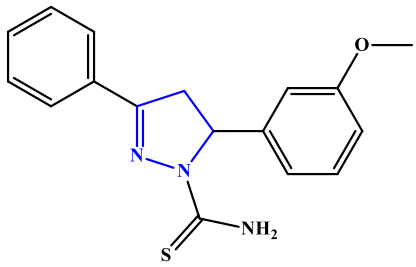

8

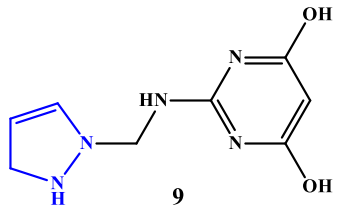

9

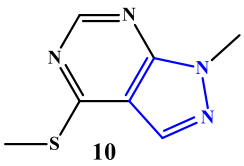

10

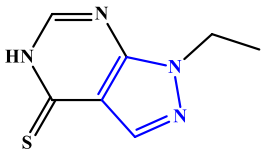

11

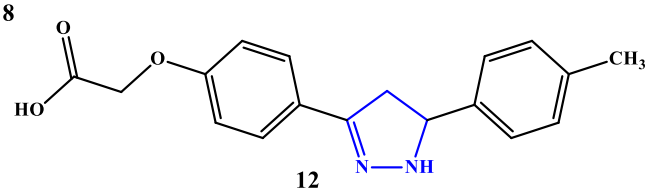

12

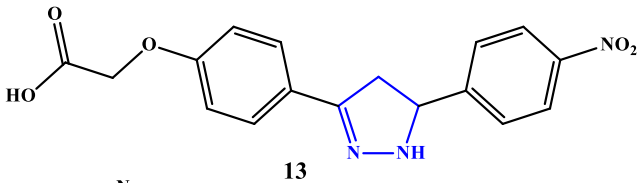

13

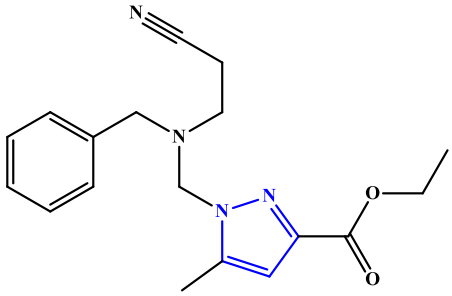

14

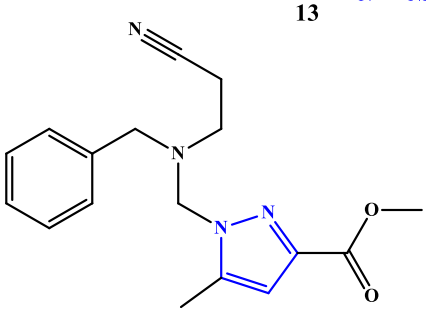

15

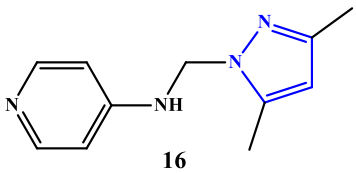

16

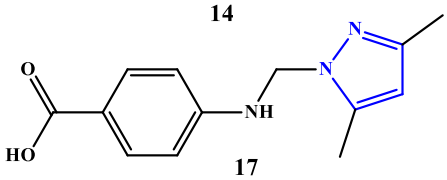

17

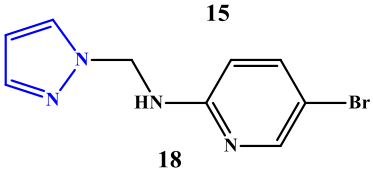

18

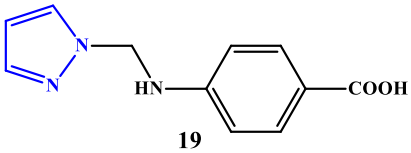

19

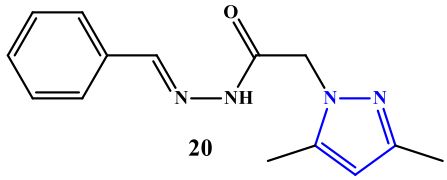

20

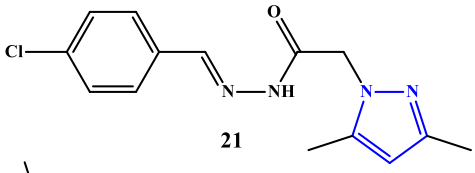

21

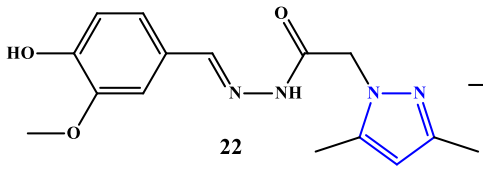

22

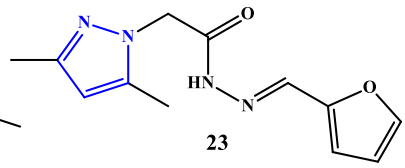

23

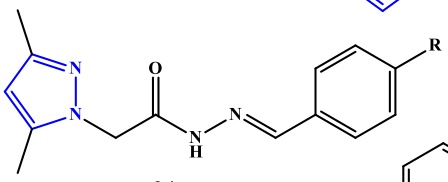

24: R = –N(CH$_3$)$_2$
25: R = –CH$_3$
26: R = –F

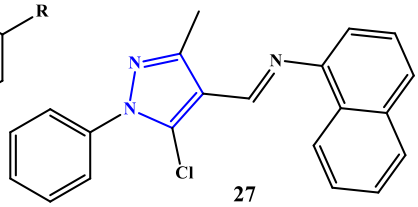

27

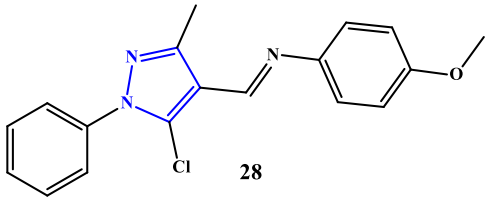

28

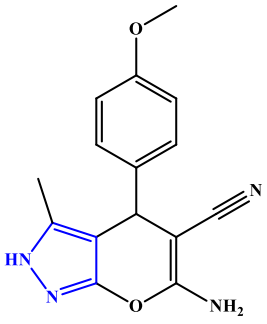

29

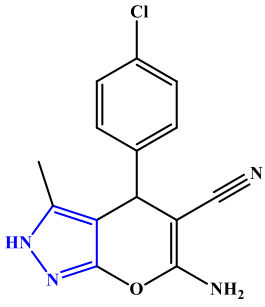

30

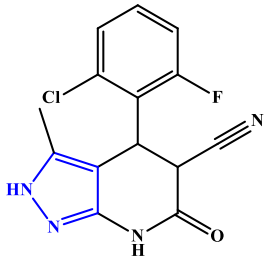

31

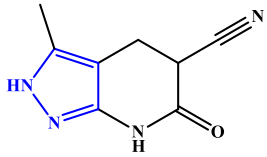

32

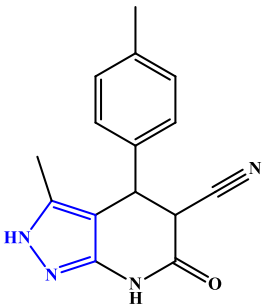

33

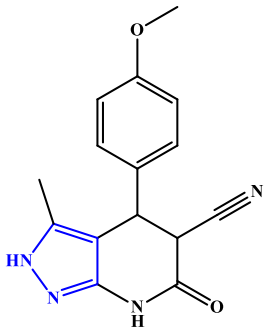

34

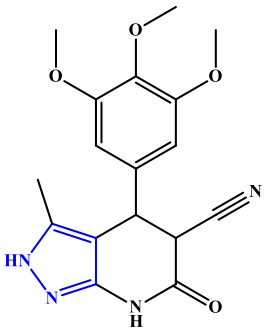

35

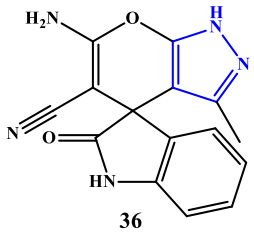

36

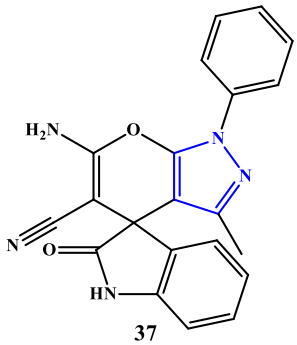

37

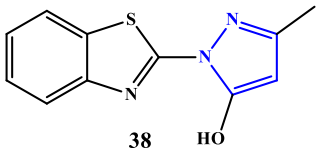

38

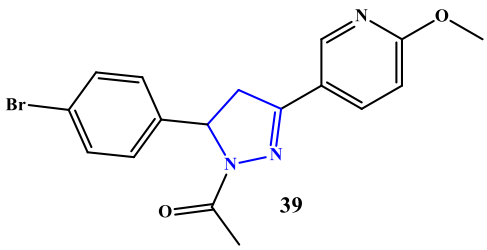

39

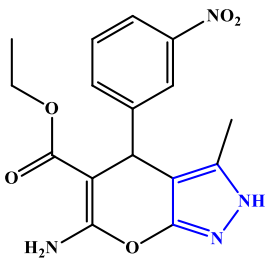

40

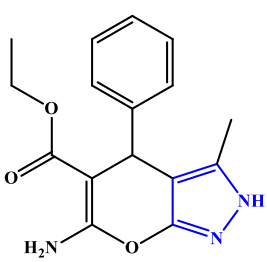

41

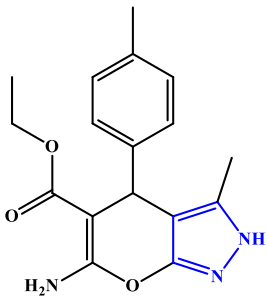

42

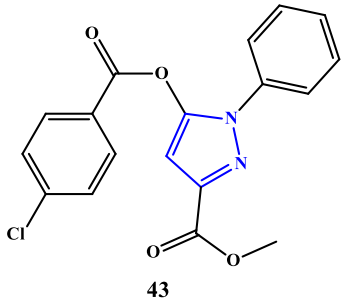

43

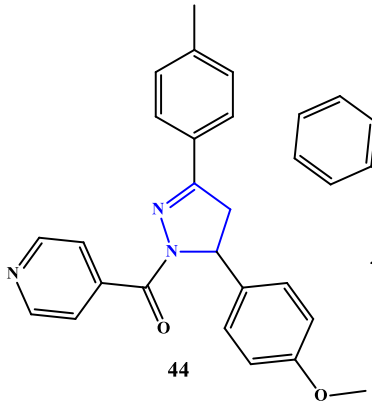

44

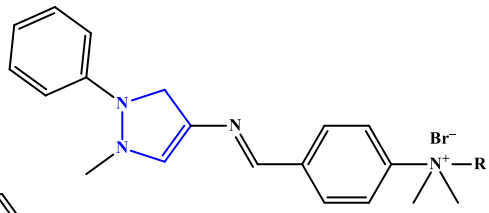

45: R = $(CH_2)_7CH_3$
46: R = $(CH_2)_{11}CH_3$
47: R = $(CH_2)_{15}CH_3$

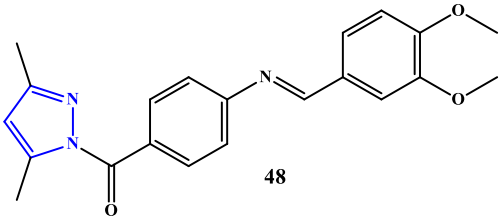

48

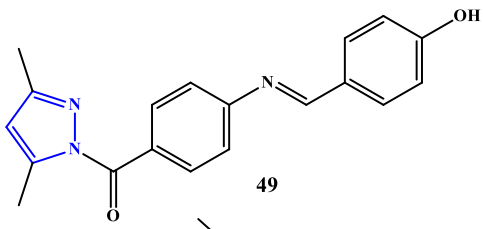

49

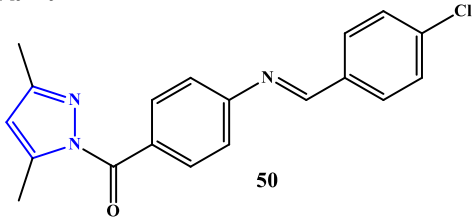

50

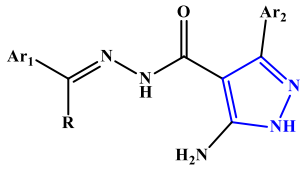

51
Ar_1 = *p*-CH_3 OPh
Ar_2 = *p*-CH_3 OPh
R = CH_3

52
Ar_1 = *p*-Cl Ph
Ar_2 = *p*-Cl Ph
R = H

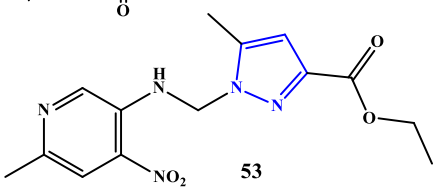

53

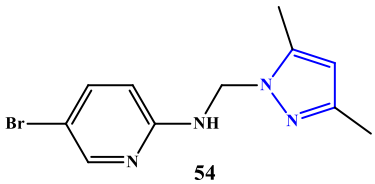

54

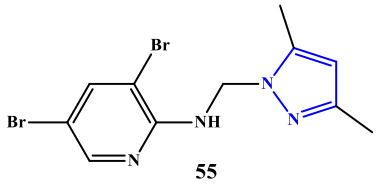

55

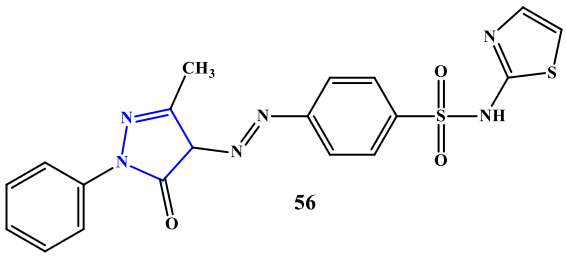

56

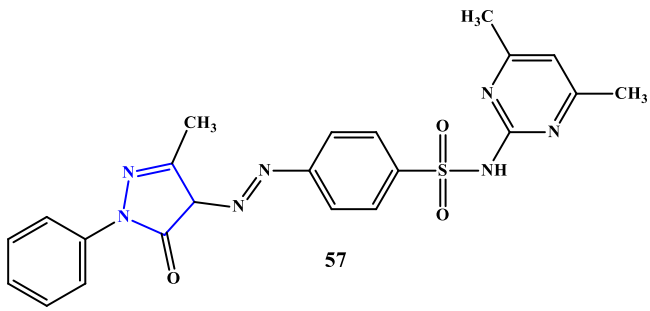

57

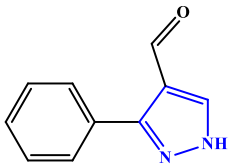

58

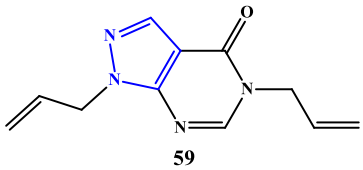

59

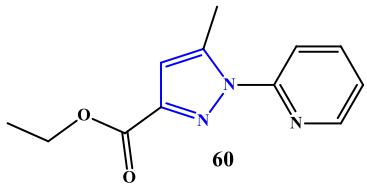

60

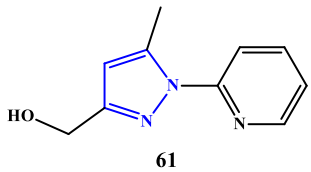

61

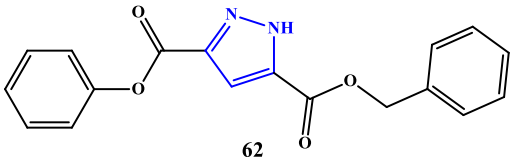

62

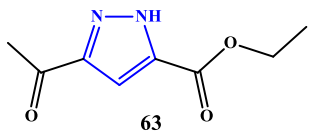

63

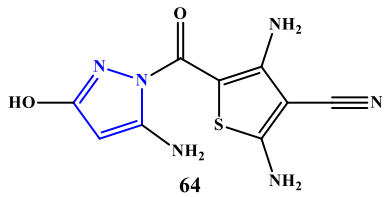

64

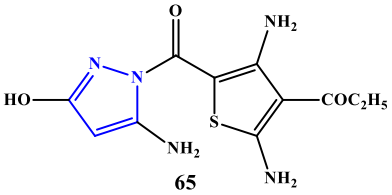

65

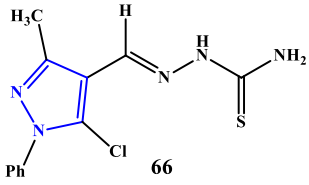

66

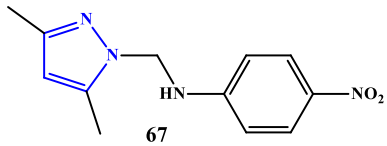

67

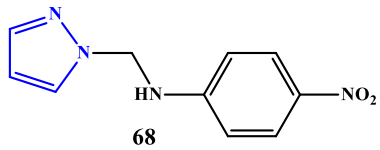

68

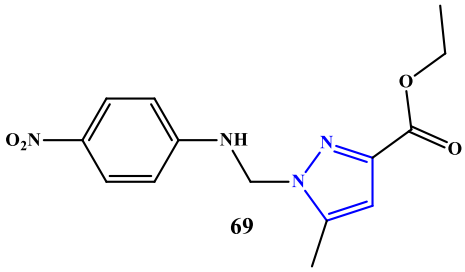

69

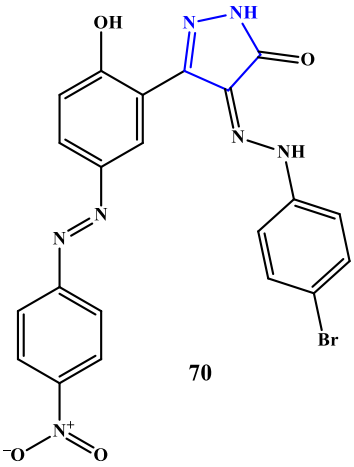

70

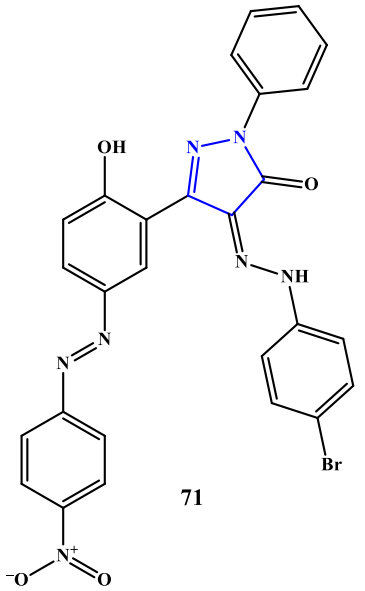

71

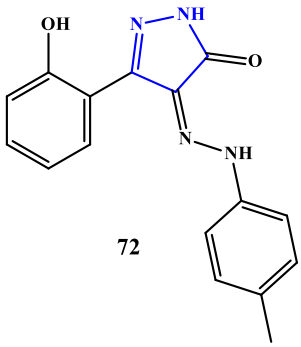

72

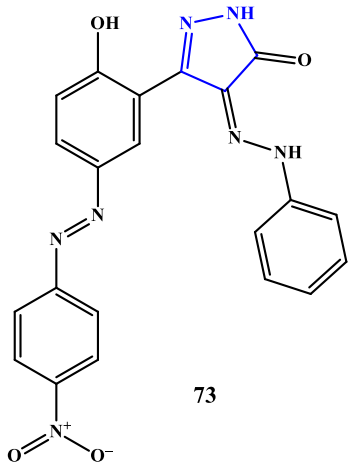

73

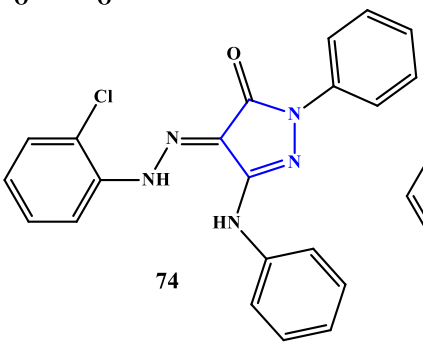

74

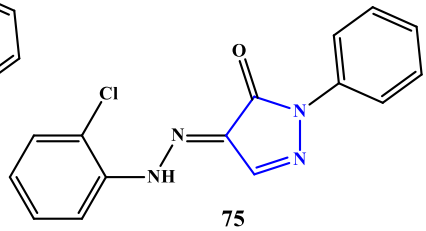

75

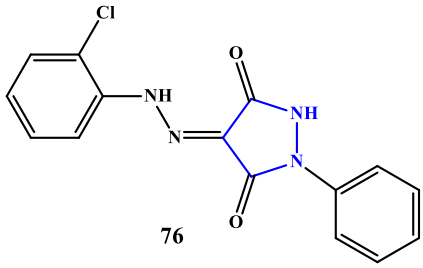

76

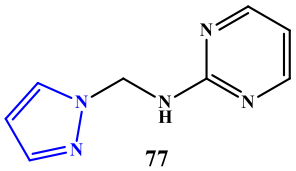

77

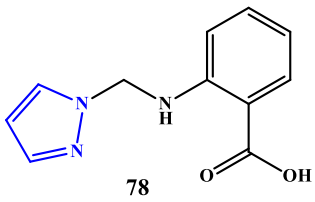

78

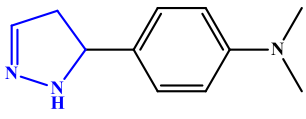

79

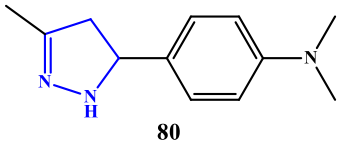

80

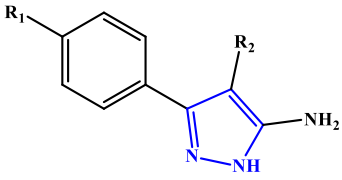

81: R_1 = H; R_2 = H
82: R_1 = H; R_2 = Br
83: R_1 = H; R_2 = CN
84: R_1 = CH_3; R_2 = H
85: R_1 = CH_3; R_2 = Br
86: R_1 = CH_3; R_2 = CN
87: R_1 = CH_3–O–; R_2 = H
88: R_1 = CH_3–O–; R_2 = Br
89: R_1 = CH_3–O–; R_2 = CN

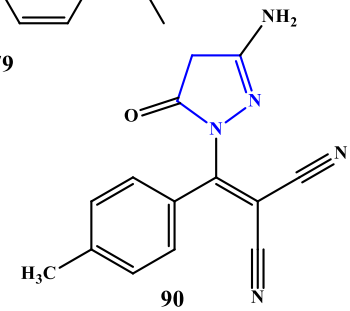

90

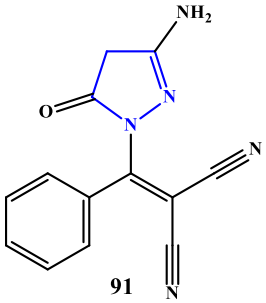

91

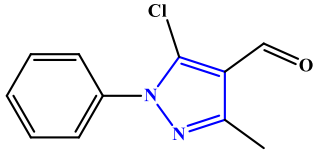

92

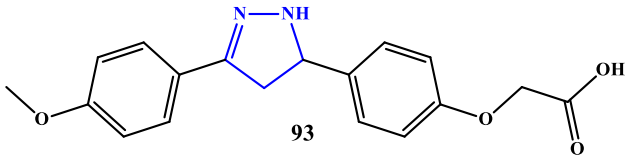

93

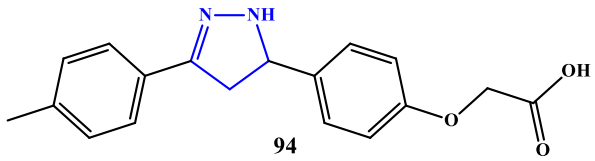

94

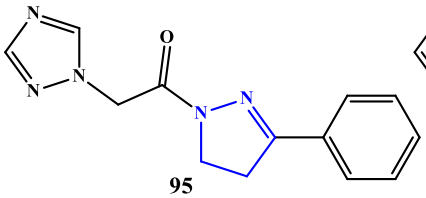

95

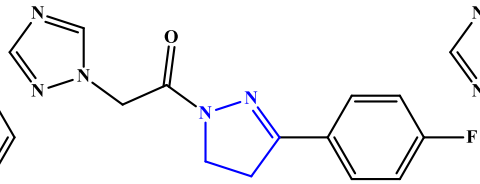

96

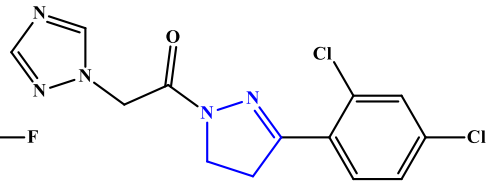

97

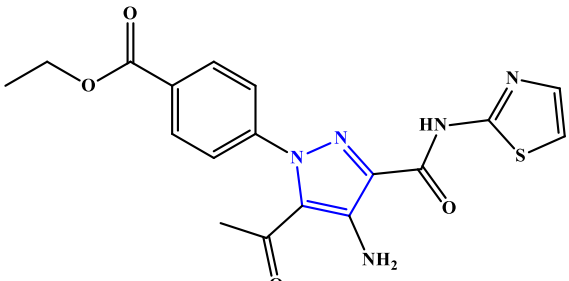

98

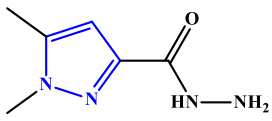

99

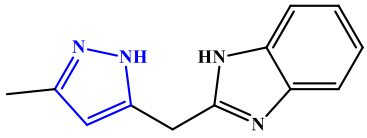

100

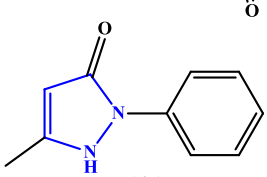

101

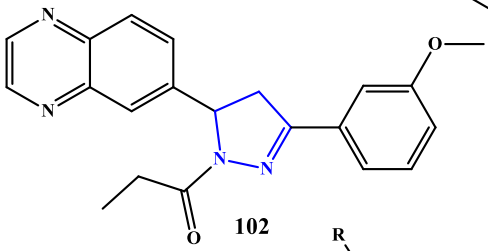

102

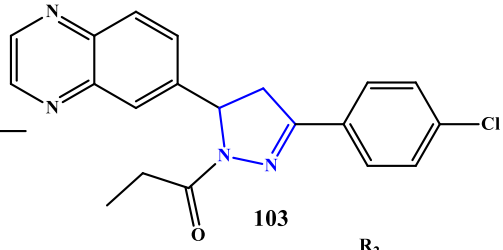

103

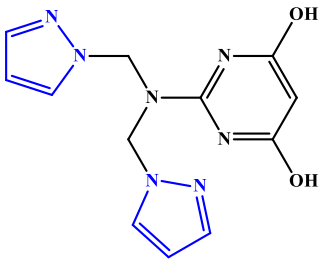

104

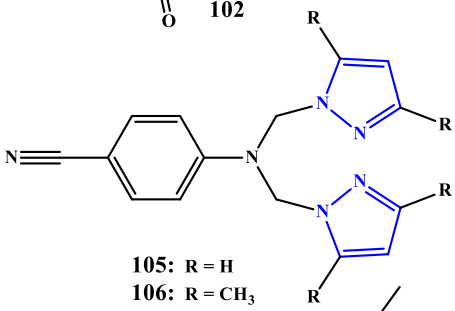

105: R = H
106: R = CH_3

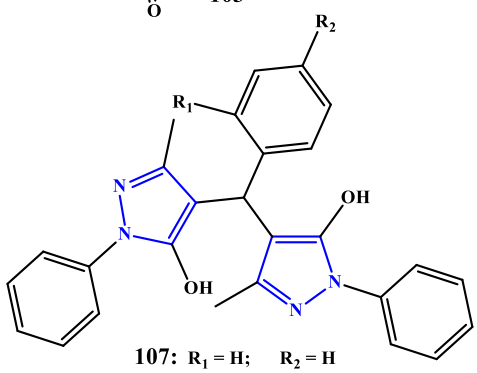

107: R_1 = H; R_2 = H
108: R_1 = H; R_2 = NO_2
109: R_1 = H; R_2 = OH
110: R_1 = OH; R_2 = OMe

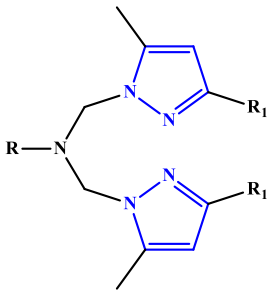

111: R =  ; R_1 = CH_3
112: R = $OH(CH_2)_2$; R_1 = CH_3
113: R = $–CH_2=CH(CH_2)$; R_1 = CH_3
114: R =  ; R_1 = COOEt
115: R = $–CH_2–C_6H_5$; R_1 = CH_3
116: R = $–(CH_3)_2N–C_6H_5$; R_1 = CH_3
117: R = $–C_6H_5$; R_1 = CH_3

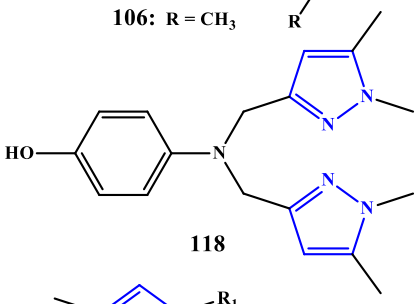

118

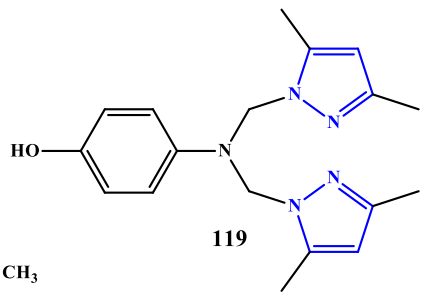

119

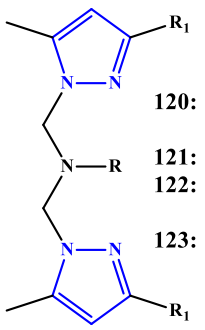

120: R =  ; R_1 = CH_3
121: R = $–CH_2CH_2OH$; R_1 = CH_3
122: R = $–CH_2CH=CH_2$; R_1 = CH_3
123: R =  ; R_1 = $COOC_2H_5$

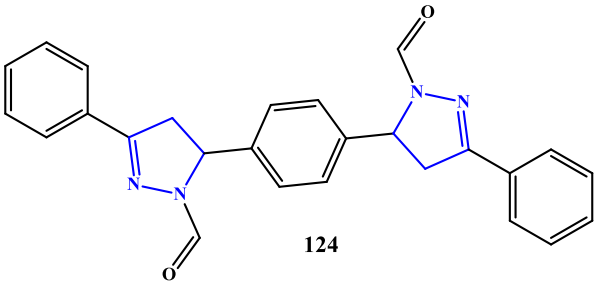

124

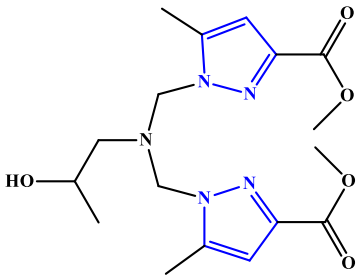

125

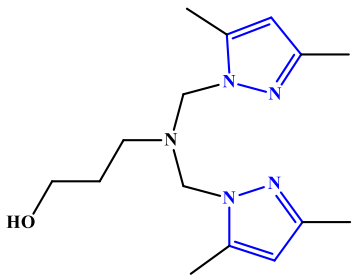

126

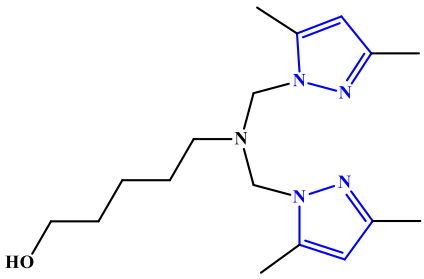

127

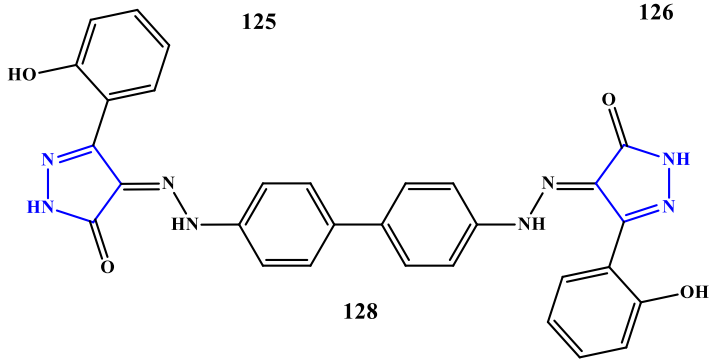

128

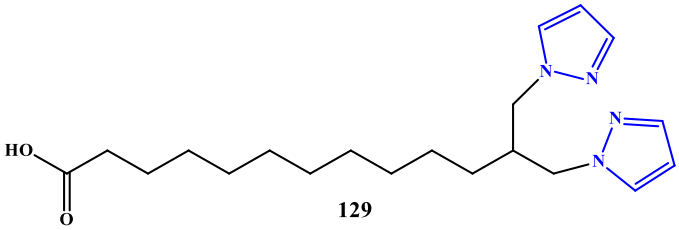

129

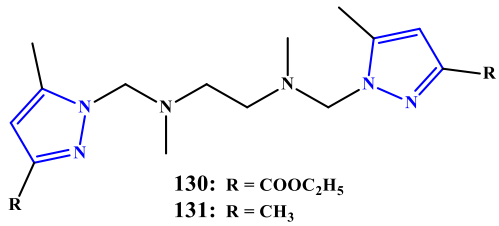

130: R = $COOC_2H_5$
131: R = CH_3

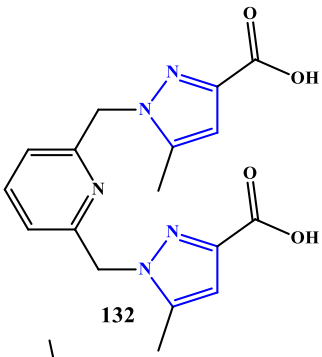

132

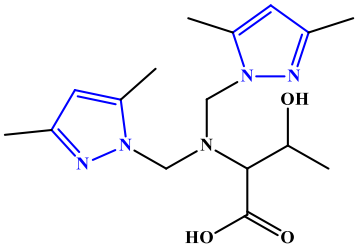

133

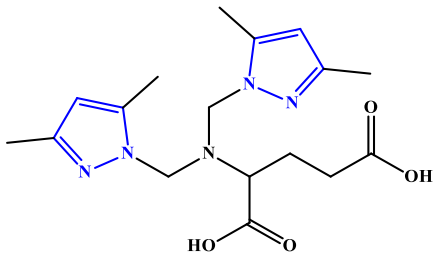

134

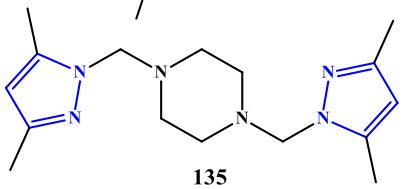

135

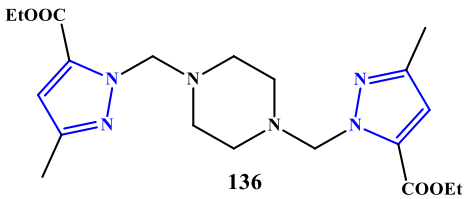

136

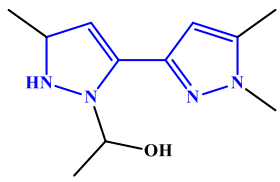

137

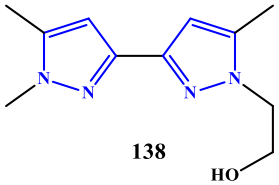

138

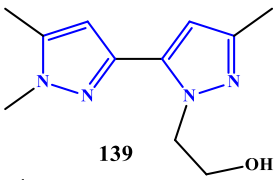

139

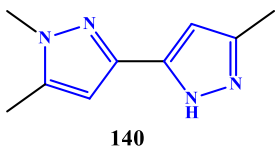

140

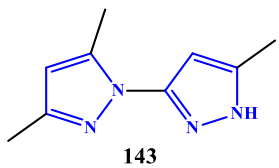

143

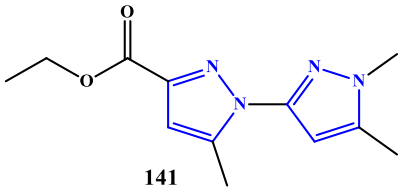

141

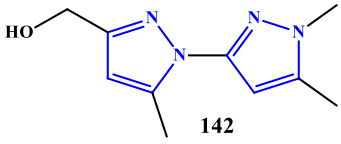

142

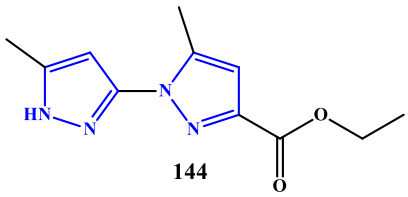

144

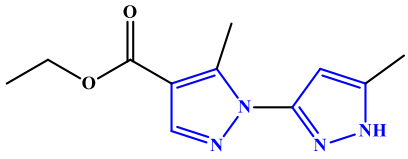

145

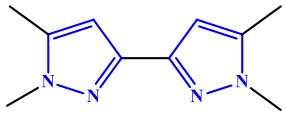

146

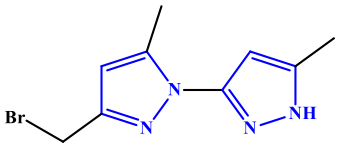

147

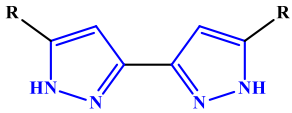

148: R = $-CH_2CH_2CH_3$

149: R =

150: R =

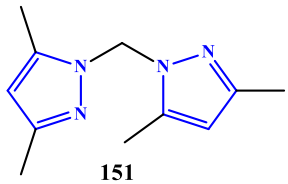

151

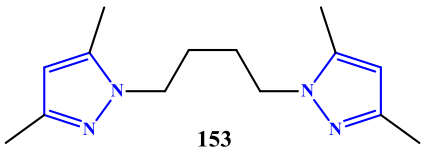

153

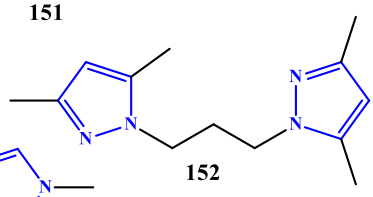

152

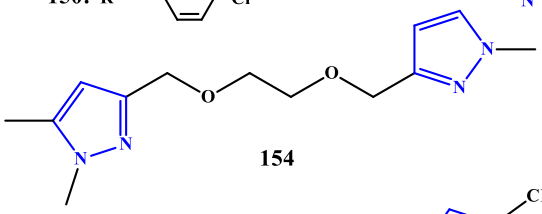

154

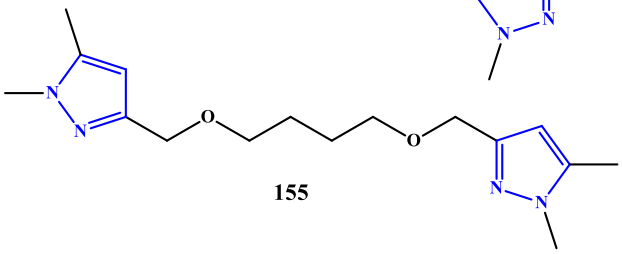

155

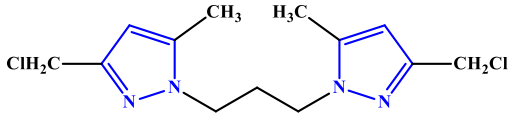

156

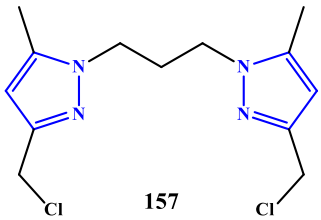

157

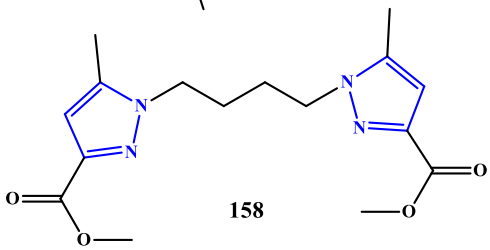

158

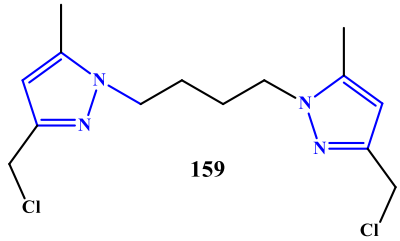

159

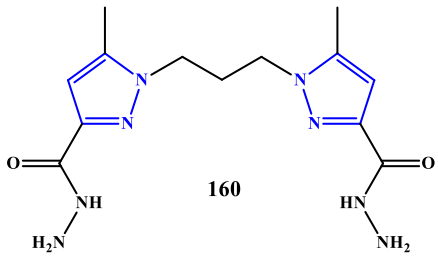

160

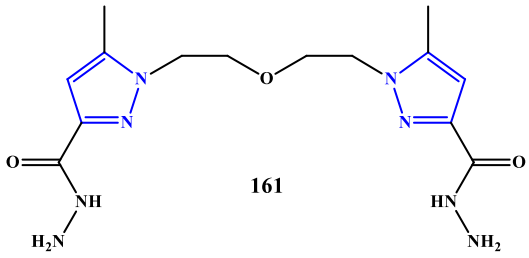

161

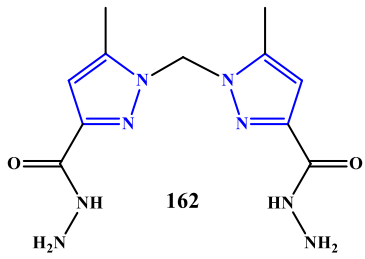

162

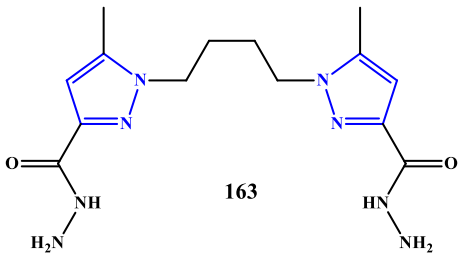

163

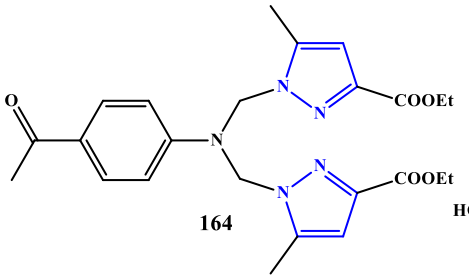

164

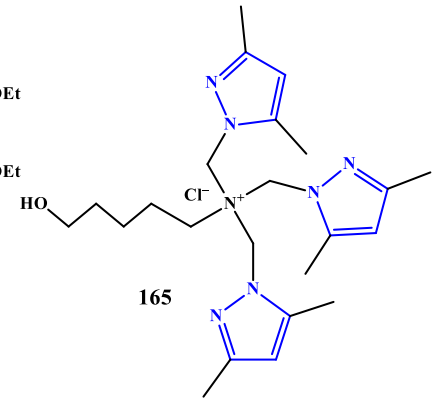

165

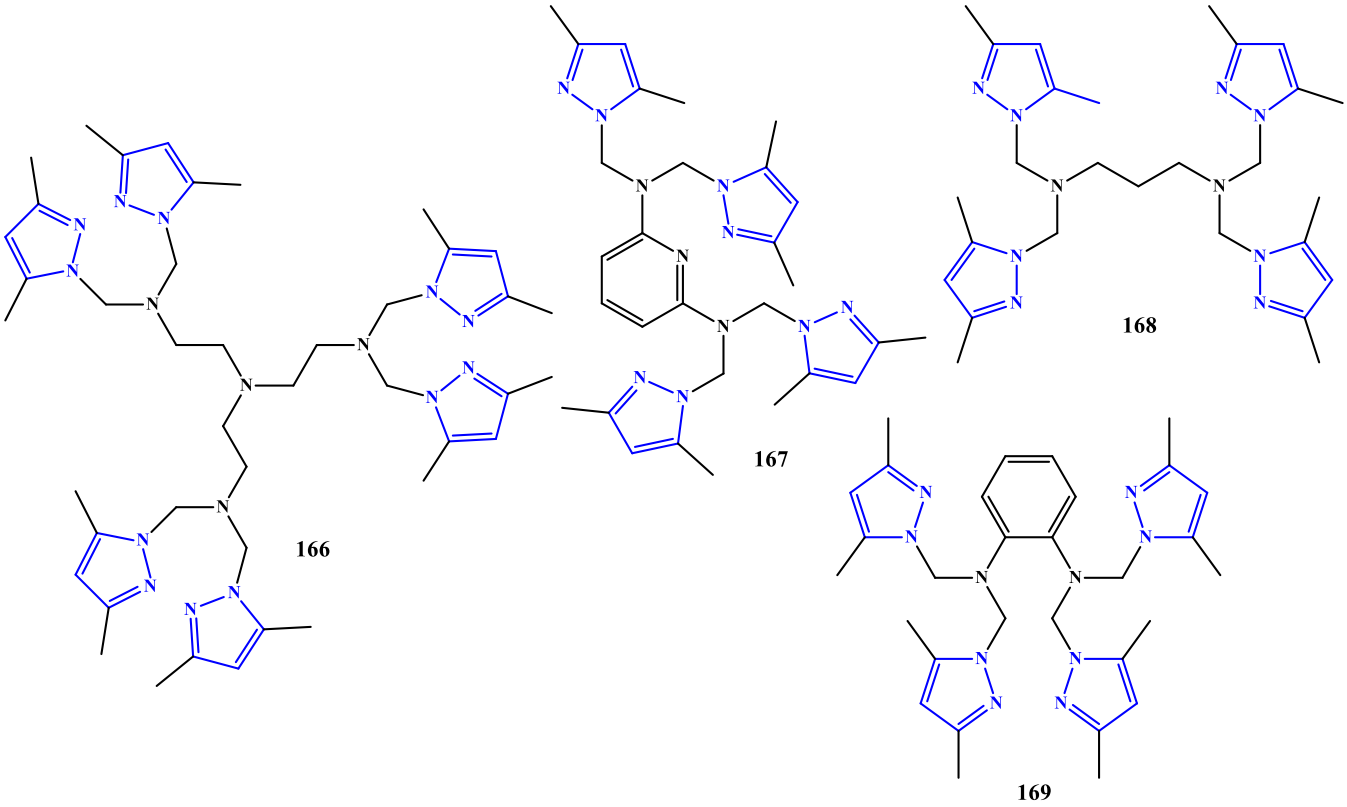

Structure of compounds **1-169**

Corrosion inhibition behaviour of heterocyclic compounds containing more than two pyrazole rings: The inhibitory efficiency of three pyrazole arms *via* methylene bridges derivative, 5-{tri-[(1,5-dimethyl-1*H*-pyrazol-3-yl)methyl]-ammonium chloride} (**165**) as corrosion inhibitor on steel material in HCl medium was also investigated [88]. According to the outcomes, tripyrazole displayed a high-level protection of 87%, whereas bipyrazole displayed 82% protection efficiency at 10^{-3} M concentration. The charge density acquired by the active centers available for adsorption and molecule size determines the corrosion mitigation performance of the compounds.

El Arrouji *et al.* [107] evaluated N^1,N^1-*bis*(2-(*bis*((3,5-dimethyl-1*H*-pyrazol-1-yl)methyl)amino)ethyl)-N^2,N^2-*bis*-((3,5-dimethyl-1H-pyrazol-1-yl)methyl)ethane-1,2-diamine (**166**) as novel corrosion inhibitor for mild steel in 1.0 M HCl and reported consistent results from multiple techniques. The polarization studies indicated mixed-type inhibition with 86% efficiency and adsorption conformed to the Langmuir model.

Timoudan *et al.* [108] investigated the corrosion inhibition performance of *N*,*N*,*N*′,*N*′-*tetra-kis*((3,5-dimethyl-1*H*-pyrazol-1-yl)methyl)pyridine-2,6-diamine (**167**) in 1.0 M HCl at 303 K. Various experimental techniques including PDP, EIS, SEM-EDX, contact angle, FTIR, XPS, XRD, UV-visible and AFM were employed for conducting the measurements. Also, the DFT and MD simulations were analysed in order to support these experimental results. Compound **167** exhibited high inhibition efficiency of 97.2% at 10^{-3} M. Polarization results confirmed mixed-type inhibition and adsorption on the carbon steel surface followed the Langmuir isotherm, indicating strong surface interaction.

Similarly, the corrosion inhibition performance of N^1,N^1,N^3,N^3-*tetrakis*-(3,5-dimethyl-1*H*-pyrazol-1-yl)methyl)propane-1,3-diamine (**168**) and N^1,N^1,N^2,N^2-*tetrakis*((3,5-dimethyl-1*H*-pyrazol-1-yl)methyl)benzene-1,2-diamine (**169**) for mild steel in 1.0 M HCl was evaluated using weight loss and electrochemical techniques [109]. Both compounds showed the mixed-type inhibition behaviour, though predominantly affecting the cathodic process. Their adsorption followed the Langmuir isotherm, with inhibition efficiencies of 87% for **168** and 94.2% for **169**. Quantum chemical calculations also indicated that electron donation and acceptance abilities increased in the order **168** < **169**, consistent with the experimental results.

Benefits of using pyrazoles as corrosion inhibitors: It has been shown that pyrazoles have superior adsorption properties over conventional inhibitors. Due to their diverse structures and functional groups, heterocyclic pyrazole compounds can be used to develop corrosion inhibitors specifically adapted to different metal types and environmental conditions due to the presence of multiple nitrogen donor atoms and π-electron systems, which facilitate the effective interaction with metal surfaces. Their structural diversity and ease of functionalization enable the design of tailored inhibitors suitable for different metals and corrosive environments. Compared with many conventional corrosion inhibitors, pyrazole derivatives are relatively accessible and can be synthesized through straightforward procedures. Their structural flexibility and potential for environmentally benign design make them

attractive for industries aiming for cost-effective and sustainable corrosion control strategies. By forming stable protective films on the metal surfaces, these compounds contribute to prolonged service life of equipment and reduced maintenance or replacement costs. Furthermore, recent progress in green and microwave-assisted synthesis, along with computational design strategies, has enabled the development of pyrazole inhibitors using safer and more sustainable methods. These approaches reduce toxic waste while enhancing inhibitor stability, efficiency and suitability for industrial applications.

Mechanism of corrosion inhibition by pyrazole compounds in acidic media: The corrosion inhibition of metals in acidic media by pyrazole compounds mainly occurs through their adsorption onto the metal surface and the subsequent formation of a protective layer. These molecules can attach to the surface by physical adsorption (physisorption), chemical adsorption (chemisorption), or a combination of both, depending on their structure, the type of metal, and conditions such as temperature. In chemisorption, the nitrogen atoms in the pyrazole ring donate electron density to the vacant *d*-orbitals of the metal, forming strong coordinate bonds. In some cases, electron back-donation from the metal to the inhibitor further stabilizes this interaction. In contrast, physisorption involves weaker electrostatic attraction, often between protonated inhibitor molecules and negatively charged ions (such as chloride) present in the acidic solution. Once adsorbed, the inhibitor molecules form a thin protective film over the metal surface. This film acts as a barrier that limits contact between the metal and aggressive species, thereby reducing both metal dissolution and hydrogen evolution reactions. The presence of heteroatoms in the pyrazole structure enhances electron distribution and improves the adsorption strength, ultimately lowering the corrosion rate. The explanation of this mechanism is clearly illustrated in Fig. 1 for better understanding.

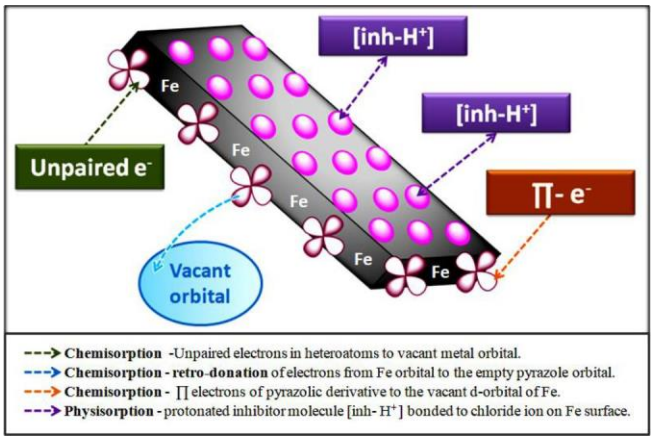

Fig. 1. Corrosion inhibition mechanism in HCl medium

Conclusion

This review comprehensively summarizes the formation of protective films by various pyrazole derivatives on iron in HCl medium for corrosion control. Inhibition performance was evaluated using weight loss (WL), potentiodynamic polarization (PDP) and electrochemical impedance spectroscopy (EIS). The effectiveness of pyrazole inhibitors is strongly influenced by concentration, immersion time and temperature. Their action mainly arises from adsorption on the metal surface, where pyrazole molecules block active corrosion sites and form a protective barrier. Most adsorption data fit the Langmuir isotherm, while some derivatives follow Temkin (**2**, **88**, **89**), Frumkin (**3**, **60**, **61**, **156**) and El-Awady (**9**, **10**) models. Compounds **25-27** conform to both Frumkin and Temkin isotherms. Polarization studies show that pyrazole derivatives generally act as mixed-type inhibitors, suppressing both anodic iron dissolution and cathodic hydrogen evolution, although certain compounds show preferential anodic or cathodic behaviour. Simultaneously the quantum chemical (DFT) results demonstrate strong agreement with experimental findings. In general, most of the *bis*-pyrazole derivatives exhibit inhibition efficiencies above 90%, whereas tris- and *tetrakis*-pyrazoles typically show efficiencies above 80%. This indicates that the number of pyrazole units significantly affects performance. *Bis*-pyrazoles generally provide superior protection, while the multi-pyrazole systems remain effective but slightly less efficient. In contrast, single pyrazole derivatives display a wider range of efficiencies. These observations highlight the importance of molecular architecture in optimizing corrosion inhibitor design.

CONFLICT OF INTEREST

The authors declare that there is no conflict of interests regarding the publication of this article.

DECLARATION OF AI-ASSISTED TECHNOLOGIES

During the preparation of this manuscript, the authors used an AI-assisted tool(s) to improve the language. The authors reviewed and edited the content and take full responsibility for the published work.

REFERENCES

1. K. Pooja, N. Tarannum and P. Chaudhary, *Discov. Mater.*, **5**, 35 (2025); https://doi.org/10.1007/s43939-025-00226-6
2. J. Hu, Z. He and X. Liu, *Materials*, **17**, 985 (2024); https://doi.org/10.3390/ma17050985
3. Y. Chen, C. Ye, X. Chen, Q. Zhai and H. Hu, *Metals*, **14**, 175 (2024); https://doi.org/10.3390/met14020175
4. K.A. Dell, Metallurgy Theory and Practical Textbook, American Technical Society, p. 351 (1989).
5. V.B. John, Introduction to Engineering Materials, Macmillan Publishing Company Ltd., edn 2, p. 321 (1980).
6. W.F. Smith, Principles of Materials Science and Engineering, McGraw-Hill (1990).
7. N. Punitha, R. Ganapathi Sundaram, G. Vengatesh, R. Rengasamy and J. Elangovan, *Inorg. Chem. Commun.*, **153**, 110732 (2023); https://doi.org/10.1016/j.inoche.2023.110732
8. B. Díaz, B. Grgur and J. Wang, *Metals*, **14**, 1194 (2024); https://doi.org/10.3390/met14101194
9. B. Hou, X. Li, X. Ma, C. Du, D. Zhang, M. Zheng, W. Xu, D. Lu and F. Ma, *npj Mater. Degrad.*, **1**, 4 (2017); https://doi.org/10.1038/s41529-017-0005-2
10. P. Bai, H. Zhao, S. Zheng and C. Chen, *Corros. Sci.*, **93**, 109 (2015); https://doi.org/10.1016/j.corsci.2015.01.024
11. D.K. Yadav and M.A. Quraishi, *Ind. Eng. Chem. Res.*, **51**, 8194 (2012); https://doi.org/10.1021/ie3002155
12. F. Bentiss, M. Traisnel and M. Lagrenee, *Corros. Sci.*, **42**, 127 (2000); https://doi.org/10.1016/S0010-938X(99)00049-9
13. R. Ganapathi Sundaram, M. Sundaravadivelu, G. Karthik and G. Vengatesh, *J. Chem. Pharm. Res.*, **7**, 823 (2015).

14. K. Bekkouch, A. Aouniti, B. Hammouti and S. Kertit, *J. Chim. Phys.*, **96**, 838 (1999); https://doi.org/10.1051/jcp:1999174
15. S. Kertit, B. Hammouti, M. Taleb and M. Brighli, *Bull. Electrochem.*, **13**, 241 (1997).
16. N. Punitha, M. Mangalam, K. Vijayalakshmi and C.S.A. Selvan, *Int. J. Nano Corros. Sci. Eng.*, **2**, 78 (2015).
17. N. Punitha and A.P. Priya, *Chem. Data Collect.*, **54**, 101172 (2024); https://doi.org/10.1016/j.cdc.2024.101172
18. G. Vengatesh, R. Ganapathi Sundaram and N. Punitha, *J. Mol. Liq.*, **410**, 125653 (2024); https://doi.org/10.1016/j.molliq.2024.125653
19. N. Punitha, R. Ganapathi Sundaram, K. Vijayalakshmi, R. Rengasamy and J. Elangovan, *J. Indian Chem. Soc.*, **99**, 100667 (2022); https://doi.org/10.1016/j.jics.2022.100667
20. M. El Boutaybi, A. Taleb, R. Touzani and Z. Bahari, *Arab. J. Chem. Environ. Res.*, **7**, 1 (2020).
21. I. Boldog, E.B. Rusanov, J. Sieler, S. Blaurock and K.V. Domasevitch, *Chem. Commun.*, **6**, 740 (2003); https://doi.org/10.1039/b212540d
22. N. Punitha, R. Ganapathi Sundaram, R. Rengasamy and J. Elangovan, *Chem. Data Collect.*, **41**, 100936 (2022); https://doi.org/10.1016/j.cdc.2022.100936
23. S.S. Abdel-Rehim, K.F. Khaled and N.A. Al-Mobarak, *Arab. J. Chem.*, **4**, 333 (2011); https://doi.org/10.1016/j.arabjc.2010.06.056
24. K.F. Khaled and S.S. Abdel-Rehim, *Arab. J. Chem.*, **4**, 397 (2011); https://doi.org/10.1016/j.arabjc.2010.07.006
25. M. Bouklah, A. Attayibat, B. Hammouti, A. Ramdani, S. Radi and M. Benkaddour, *Appl. Surf. Sci.*, **240**, 341 (2005); https://doi.org/10.1016/j.apsusc.2004.07.001
26. F. Touham, A. Aouniti, Y. Abed, B. Hammouti, S. Kertit and A. Ramdani, *Bull. Electrochem.*, **16**, 245 (2000).
27. A. Sehmi, H.B. Ouici, A. Guendouzi, M. Ferhat, O. Benali and F. Boudjellal, *J. Electrochem. Soc.*, **167**, 155508 (2020); https://doi.org/10.1149/1945-7111/abab25
28. F. Boudjellal, H.B. Ouici, A. Guendouzi, O. Benali and A. Sehmi, *J. Mol. Struct.*, **1199**, 127051 (2020); https://doi.org/10.1016/j.molstruc.2019.127051
29. H.B. Ouici, O. Benali and A. Guendouzi, *Res. Chem. Intermed.*, **42**, 7085 (2016); https://doi.org/10.1007/s11164-016-2520-0
30. J. Bouhoud, M. El Fal, Y. Ramli, A. Bellaouchou and E.M. Essassi, *J. Mater. Environ. Sci.*, **8**, 1935 (2017); https://doi.org/10.26872/jmes.2018.9.2.49
31. L. El Hattabi, S. Echihi, M. El Fal, E.M. Essassi and M. Tabyaoui, *J. Mater. Environ. Sci.*, **8**, 2428 (2017).
32. H. Lgaz, R. Salghi, A. Chaouiki, S. Shubhalaxmi, S. Jodeh and K. Subrahmanya Bhat, *Cogent Eng.*, **5**, 1441585 (2018); https://doi.org/10.1080/23311916.2018.1441585
33. L. Herrag, A. Chetouani, S. Elkadiri, B. Hammouti and A. Aouniti, *Port. Electrochem. Acta*, **26**, 211 (2007); https://doi.org/10.4152/pea.200802211
34. F. El Hajjaji, F. Abrigach, O. Hamed, A.R. Hasan, M. Taleb, S. Jodeh, E. Rodríguez-Castellón, M.V. Martínez de Yuso and M. Algarra, *Coatings*, **8**, 330 (2018); https://doi.org/10.3390/coatings8100330
35. H. Bouammali, F. Abrigach, S. Jerdioui, B. El-Haitout, A. Aouniti, R. Touzani, B. Hammouti and R. Salghi, *Int. J. Corros. Scale Inhib.*, **13**, 367 (2024); https://doi.org/10.17675/2305-6894-2024-13-1-19
36. S. El Arrouji, K. Karrouchi, A. Berisha, K. Ismaily Alaoui, I. Warad, Z. Rais, S. Radi, M. Taleb, M. Ansar and A. Zarrouk, *Colloids Surf. A Physicochem. Eng. Asp.*, **604**, 125325 (2020); https://doi.org/10.1016/j.colsurfa.2020.125325
37. S.E. Arrouji, K. Karrouchi, I. Warad, A. Berisha, K.I. Alaoui, Z. Rais, S. Radi, M. Taleb, M. Ansar and A. Zarrouk, *Chem. Data Collect*, **40**, 100885 (2022); https://doi.org/10.1016/j.cdc.2022.100885
38. S.A. Mrani, S. El Arrouji, K. Karrouchi, F. El Hajjaji, K.I. Alaoui, Z. Rais and M. Taleb, *Int. J. Corros. Scale Inhib.*, **7**, 542 (2018).
39. R. Khanna, V. Kalia, R. Kumar, R. Kumar, P. Kumar, H. Dahiya, P. Pahuja, G. Jhaa and H. Kumar, *J. Mol. Struct.*, **1297**, 136845 (2024); https://doi.org/10.1016/j.molstruc.2023.136845
40. M. Yadav, L. Gope, N. Kumari and P. Yadav, *J. Mol. Liq.*, **216**, 78 (2016); https://doi.org/10.1016/j.molliq.2015.12.106
41. A. Dandia, S.L. Gupta, P. Singh and M.A. Quraishi, *ACS Sustain. Chem.& Eng.*, **1**, 1303 (2013); https://doi.org/10.1021/sc400155u
42. N.K. Gupta, J. Haque, R. Salghi, H. Lgaz, A.K. Mukherjee and M.A. Quraishi, *J. Bio Tribocorros.*, **4**, 16 (2018); https://doi.org/10.1007/s40735-018-0132-5
43. C.E.B. Maia, G.A. Romeiro, M.C.C. Veloso, B.S. Peixoto and R.V. Rodrigues, *Rev. Virtual Quim.*, **10**, 102 (2018); https://doi.org/10.21577/1984-6835.20180010
44. P. Shekara, J. Kudva, R. Sadashiva, D. Naral, P.R. Dsouza and N.A. Shetty, *ChemistrySelect*, **8**, e202300448 (2023); https://doi.org/10.1002/slct.202300448
45. P. Dohare, K.R. Ansari, M.A. Quraishi and I.B. Obot, *J. Ind. Eng. Chem.*, **52**, 197 (2017); https://doi.org/10.1016/j.jiec.2017.03.044
46. M. Yadav, R.R. Sinha, T.K. Sarkar and N. Tiwari, *J. Adhes. Sci. Technol.*, **29**, 1690 (2015); https://doi.org/10.1080/01694243.2015.1040979
47. S.M. Tawfik, *J. Mol. Liq.*, **207**, 185 (2015); https://doi.org/10.1016/j.molliq.2015.03.036
48. A. Shareef Jasim, A.A. Khadom, K.H. Rashid and K.F. AL-Azawi, *Results Chem.*, **4**, 100569 (2022); https://doi.org/10.1016/j.rechem.2022.100569
49. A.S. Jasim, K.H. Rashid, K.F. AL-Azawi and A.A. Khadom, *Results Eng.*, **15**, 100573 (2022); https://doi.org/10.1016/j.rineng.2022.100573
50. K.H. Rashid, K.F. AL-Azawi, A.A. Khadom, A.S. Jasim and M.M. Kadhim, *J. Mol. Struct.*, **1287**, 135661 (2023); https://doi.org/10.1016/j.molstruc.2023.135661
51. P.K. Paul, M. Yadav and I.B. Obot, *J. Mol. Liq.*, **314**, 113513 (2020); https://doi.org/10.1016/j.molliq.2020.113513
52. G. Laadam, F. Benhiba, M. El Faydy, A. Titi, A.S. Al-Gorair, M. Alshareef, H. Hawsawi, R. Touzani, I. Warad, A. Bellaouchou, A. Guenbour, M. Abdallah and A. Zarrouk, *Inorg. Chem. Commun.*, **145**, 109963 (2022); https://doi.org/10.1016/j.inoche.2022.109963
53. K. Ismaily Alaoui, F. El Hajjaji, M.A. Azaroual, M. Taleb, A. Chetouani, B. Hammouti, F. Abrigach, M. Khoutoul, Y. Abboud, A. Aouniti and R. Touzani, *J. Chem. Pharm. Res.*, **6**, 63 (2014).
54. A.M. Ashmawy, M.A. Mostafa, A.B. Kamal, G.A.M. Ali and M.S.A. El-Gaby, *Sci. Rep.*, **13**, 18555 (2023); https://doi.org/10.1038/s41598-023-45659-2
55. Y.E.L. Aoufir, H. Lgaz, K. Toumiat, R. Salghi, S. Jodeh, M. Zougagh, A. Guenbour and H. Oudda, *Res. J. Pharm. Biol. Chem. Sci.*, **7**, 1219 (2016).
56. M. Boudalia, R.M. Fernández-Domene, L. Guo, S. Echihi, M.E. Belghiti, A. Zarrouk, A. Bellaouchou, A. Guenbour and J. García-Antón, *Materials*, **16**, 678 (2023); https://doi.org/10.3390/ma16020678
57. K. Tebbji, H. Oudda, B. Hammouti, M. Benkaddour, M. El Kodadi and A. Ramdani, *Colloids Surf. A Physicochem. Eng. Asp.*, **259**, 143 (2005); https://doi.org/10.1016/j.colsurfa.2005.02.030
58. M.S. Motawea and M.A. Abdelaziz, *Eur. J. Chem.*, **6**, 342 (2015); https://doi.org/10.5155/eurjchem.6.3.342-349.1279
59. R.S. Abdel Hameed, H.I. Al-Shafey, A.S. Abul Magd and H.A. Shehata, *J. Mater. Environ. Sci.*, **3**, 294 (2012).
60. L. Adlani, N. Benzbiria, A. Titi, F. Benhiba, I. Warad, N. Timoudan, G. Kaichouh, A. Bellaouchou, R. Touzani, H. Zarrok, H. Oudda and A. Zarrouk, *Anal. Bioanal. Electrochem.*, **15**, 967 (2023); https://doi.org/10.22034/ABEC.2023.709114
61. L. Adlani, N. Benzbiria, A. Titi, N. Timoudan, I. Warad, A. AlObaid, B.M. Al-Maswari, F. Benhiba, R. Touzani, H. Zarrok, F. Bentiss, H. Oudda and A. Zarrouk, *ACS Omega*, **9**, 13746 (2024); https://doi.org/10.1021/acsomega.3c08282
62. M.M. Shaban, N.M. El Basiony, A.B. Radwan, E.E. El-Katori, A. Abu-Rayyan, N.H. Bahtiti and M.M. Abdou, *ACS Omega*, **8**, 30068 (2023); https://doi.org/10.1021/acsomega.3c02333
63. M.A. Abbas, A.M. Eid, M.M. Abdou, A. Elgendy, R.A. El-Saeed and E.G. Zaki, *ACS Omega*, **6**, 8894 (2021); https://doi.org/10.1021/acsomega.0c06050
64. A.E.A.S. Fouda, S.M. Rashwan, M.M. Kamel, A.H.M. Gad and K. Shalabi, *Biointerface Res. Appl. Chem.*, **11**, 14673 (2021); https://doi.org/10.33263/BRIAC116.1467314687

65. G. Laadam, M. El-Faydy, F. Benhiba, A. Titi, H. Amegroud, A.S. Al Gorair, H. Hawsawi, R. Touzani, I. Warad, A. Bellaouchou, A. Guenbour, M. Abdallah and A. Zarrouk, *J. Mol. Liq.*, **375**, 121268 (2023); https://doi.org/10.1016/j.molliq.2023.121268
66. R. Chadli, M. Elazouzi, I. Khelladi, A.M. Elhourri, H. Elmsellem, A. Aouniti, J.K. Mulengi and B. Hammouti, *Port. Electrochem. Acta*, **35**, 65 (2017); https://doi.org/10.4152/pea.201702065
67. R. Chadli, M. Elazouzi, I. Khelladi, A.M. Elhorri, J.K. Mulangi, B. Hammouti and A. Aouiniti, *Port. Electrochem. Acta*, **38**, 125 (2020); https://doi.org/10.4152/pea.202002125
68. G.M. Abu-Eienien and A.A. El-Maghraby, *J. Indian Chem. Soc.*, **77**, 473 (2000).
69. K.R. Ansari, M.A. Quraishi, A. Singh, S. Ramkumar and I.B. Obote, *RSC Adv.*, **6**, 24130 (2016); https://doi.org/10.1039/C5RA25441H
70. A. Thomas, P.R. Ammal and A. Joseph, *Chem. Pap.*, **74**, 3025 (2020); https://doi.org/10.1007/s11696-020-01142-0
71. H. Lgaz, S.K. Saha, A. Chaouiki, K.S. Bhat, R. Salghi, Shubhalaxmi, P. Banerjee, I.H. Ali, M.I. Khan and I.-M. Chung, *Constr. Build. Mater.*, **233**, 117320 (2020); https://doi.org/10.1016/j.conbuildmat.2019.117320
72. W. Li, X. Zhao, F. Liu, J. Deng and B. Hou, *Mater. Corros.*, **60**, 287 (2009); https://doi.org/10.1002/maco.200805081
73. B.A. Al Jahdaly and G.S. Masaret, *J. Mol. Liq.*, **364**, 119933 (2022); https://doi.org/10.1016/j.molliq.2022.119933
74. K. Cherrak, M.E. Belghiti, A. Berrissoul, M. El Massaoudi, M. El Faydy, M. Taleb, S. Radi, A. Zarrouk and A. Dafali, *Surf. Interfaces*, **20**, 100578 (2020); https://doi.org/10.1016/j.surfin.2020.100578
75. K. Chkirate, K. Azgaou, H. Elmsellem, B. El Ibrahimi, N.K. Sebbar, E.H. Anouar, M. Benmessaoud, S. El Hajjaji and E.M. Essassi., *J. Mol. Liq.*, **321**, 114750 (2021); https://doi.org/10.1016/j.molliq.2020.114750
76. K. Cao, W. Li and L. Yu, *Int. J. Electrochem. Sci.*, **7**, 806 (2012); https://doi.org/10.1016/S1452-3981(23)13377-3
77. L.O. Olasunkanmi and E.E. Ebenso, *J. Colloid Interface Sci.*, **561**, 104 (2020); https://doi.org/10.1016/j.jcis.2019.11.097
78. N. Arrousse, R. Salim, Y. Kaddouri, A. Zarrouk, D. Zahri, F.E. Hajjaji, R. Touzani, M. Taleb and S. Jodeh, *Arab. J. Chem.*, **13**, 5949 (2020); https://doi.org/10.1016/j.arabjc.2020.04.030
79. Y. Kaddouri, A. Takfaoui, F. Abrigach, B. Hammouti, R. Touzani and H. Sdassi, *J. Mater. Environ. Sci.*, **8**, 845 (2017).
80. C. Verma, V.S. Saji, M.A. Quraishi and E.E. Ebenso, *J. Mol. Liq.*, **298**, 111943 (2020); https://doi.org/10.1016/j.molliq.2019.111943
81. A. El Ouafi, B. Hammouti, H. Oudda, S. Kertit, R. Touzani and A. Ramdani, *Anti-Corros. Methods Mater.*, **49**, 199 (2002); https://doi.org/10.1108/00035590210426463
82. K. Tebbji, I. Bouabdellah, A. Aouniti, B. Hammouti, H. Oudda, M. Benkaddour and A. Ramdani, *Mater. Lett.*, **61**, 799 (2007); https://doi.org/10.1016/j.matlet.2006.05.063
83. K. Tebbji, A. Aouniti, M. Benkaddour, H. Oudda, I. Bouabdallah, B. Hammouti and A. Ramdani, *Prog. Org. Coat.*, **54**, 170 (2005); https://doi.org/10.1016/j.porgcoat.2005.06.001
84. K. Tebbji, H. Oudda, B. Hammouti, M. Benkaddour, M. El Kodadi, F. Malek and A. Ramdani, *Appl. Surf. Sci.*, **241**, 326 (2005); https://doi.org/10.1016/j.apsusc.2004.07.036
85. K. Laarej, M. Bouachrine, S. Radi, S. Kertit and B. Hammouti, *J. Chem.*, **7**, 419 (2010); https://doi.org/10.1155/2010/273206
86. I. Selatnia, A. Sid, M. Benahmed, O. Dammene debbih, T. Ozturk and N. Gherraf, *Prot. Met. Phys. Chem. Surf.*, **54**, 1182 (2018); https://doi.org/10.1134/S2070205118060229
87. H. Bendaha, A. Zarrouk, A. Aouniti, B. Hammouti, S. El Kadiri, R. Salghi and R. Touzani, *Phys. Chem. News*, **64**, 95 (2012).
88. M. Elayyachy, M. El Kodadi, B. Hammouti, A. Ramdani and A. El Idrissi, *Pigm. Resin Technol.*, **33**, 375 (2004); https://doi.org/10.1108/03699420410568409
89. E.E. El-Katori, R.A. El-Saeed and M.M. Abdou, *Arab. J. Chem.*, **15**, 104373 (2022); https://doi.org/10.1016/j.arabjc.2022.104373
90. Y.E. Ouadi, M. Lamsayah, H. Bendaif, F. Benhiba, R. Touzani, I. Warad and A. Zarrouk, *Chem. Data Collect.*, **31**, 100638 (2021); https://doi.org/10.1016/j.cdc.2020.100638
91. M. Bouklah, Y. Karzazi, M. Kaddouri, M.E. Belghiti, B. Hammouti, Y. Toubi, A. Aouniti, S. Radi and K. Emran, *Asian J. Chem.*, **29**, 1827 (2017); https://doi.org/10.14233/ajchem.2017.20654
92. M. El Azzouzi, A. Aouniti, M. El Massaoudi, S. Radi, B. Hammouti, M.A. Quraishi, H. Bendaif and Y. El Ouadi, *Int. J. Corros. Scale Inhib.*, **6**, 463 (2017); https://doi.org/10.17675/2305-6894-2017-6-4-6
93. H. Zarrok, A. Zarrouk, R. Salghi, R. Touzani and H. Oudda, *Pharm. Lett.*, **5**, 327 (2013).
94. A. Zarrouk, H. Zarrok, R. Salghi, N. Bouroumane, B. Hammouti, S.S. Al-Deyab and R. Touzani, *Int. J. Electrochem. Sci.*, **7**, 10215 (2012); https://doi.org/10.1016/S1452-3981(23)16271-7
95. M. Bouklah, M. Kaddouri, Y. Toubi, B. Hammouti, S. Radi and E.E. Ebenso, *Int. J. Electrochem. Sci.*, **8**, 7437 (2013); https://doi.org/10.1016/S1452-3981(23)14858-9
96. K. Tebbji, A. Aouniti, A. Attayibat, B. Hammouti, H. Oudda, M. Benkaddour, S. Radi and A. Nahle, *Indian J. Chem. Technol.*, **18**, 244 (2011).
97. M. Bouklah, B. Hammouti, M. Benkaddour, A. Attayibat and S. Radi, *Pigm. Resin Technol.*, **34**, 197 (2005); https://doi.org/10.1108/03699420510609088
98. K. Tebbji, B. Hammouti, H. Oudda, A. Ramdani and M. Benkadour, *Appl. Surf. Sci.*, **252**, 1378 (2005); https://doi.org/10.1016/j.apsusc.2005.02.097
99. H. Zarrok, H. Oudda, A. El Midaoui, A. Zarrouk, B. Hammouti, M. Ebn Touhami, A. Attayibat, S. Radi and R. Touzani, *Res. Chem. Intermed.*, **38**, 2051 (2012); https://doi.org/10.1007/s11164-012-0525-x
100. H. Zarrok, S.S. Al-Deyab, A. Zarrouk, R. Salghi, B. Hammouti, H. Oudda, M. Bouachrine and F. Bentiss, *Int. J. Electrochem. Sci.*, **7**, 4047 (2012); https://doi.org/10.1016/S1452-3981(23)19519-8
101. M. Benabdellah, R. Touzani, A. Aouniti, A. Dafali, S. El Kadiri, B. Hammouti and M. Benkaddour, *Mater. Chem. Phys.*, **105**, 373 (2007); https://doi.org/10.1016/j.matchemphys.2007.05.001
102. F. Touhami, A. Aouniti, Y. Abed, B. Hammouti, S. Kertit, A. Ramdani and K. Elkacemi, *Corros. Sci.*, **42**, 929 (2000); https://doi.org/10.1016/S0010-938X(99)00123-7
103. F. Touhami, B. Hammouti, A. Aouniti and S. Kertit, *Ann. Chim.*, **24**, 581 (1999); https://doi.org/10.1016/S0151-9107(00)86628-3
104. I. El Ouali, A. Chetouani, B. Hammouti, A. Aouniti, R. Touzani, S. El Kadiri and S. Nlate, *Port. Electrochem. Acta*, **31**, 53 (2013); https://doi.org/10.4152/pea.201302053
105. K. Cherrak, M. El Massaoudi, H. Outada, M. Taleb, H. Lgaz, A. Zarrouk, S. Radi and A. Dafali, *J. Mol. Liq.*, **342**, 117507 (2021); https://doi.org/10.1016/j.molliq.2021.117507
106. K. Cherrak, O.M.A. Khamaysa, H. Bidi, M.E. Massaoudi, I.A. Ali, S. Radi, Y. El Ouadi, F. El-Hajjaji, A. Zarrouk and A. Dafali, *J. Mol. Struct.*, **1261**, 132925 (2022); https://doi.org/10.1016/j.molstruc.2022.132925
107. S. El Arrouji, K. Ismaily Alaoui, A. Zerrouki, S. El Kadiri, R. Touzani, Z. Rais, M. Filali Baba, M. Taleb, A. Chetouani and A. Aouniti, *J. Mater. Environ. Sci.*, **7**, 299 (2016).
108. N. Timoudan, A. Titi, M. El Faydy, F. Benhiba, R. Touzani, I. Warad, A. Bellaouchou, A. Alsulmi, B. Dikici, F. Bentiss and A. Zarrouk, *Colloids Surf. A Physicochem. Eng. Asp.*, **682**, 132771 (2024); https://doi.org/10.1016/j.colsurfa.2023.132771
109. Y.E. Louadi, F. Abrigach, A. Bouyanzer, R. Touzani, A. Assyry, A. Zarrouk and B. Hammouti, *Port. Electrochem. Acta*, **35**, 159 (2017); https://doi.org/10.4152/pea.201703159